ON THE RECOMBINATION RATE OF IODINE ATOMS IN THE PRESENCE OF VARIOUS GASES

Thesis by

Rolf Engleman, Jr.

In Partial Fulfillment of the Requirements

For the Degree of

Doctor of Philosophy

California Institute of Technology

Pasadena, California

1959

To My Wife, Daughter, and Parents

Acknowledgments

I would like to express my gratitude to Professor Norman R. Davidson for suggesting and supervising my thesis research. His skillful and enthusiastic guidance has been a major factor in the completion of this thesis.

I am also indebted to the Office of Naval Research for a research assistantship and summer support (1955-56), the California Institute of Technology for two teaching assistantships (1956-58), and the Shell Oil Company for a research fellowship (1958-59).

This research was supported by the Office of Naval Research.

TABLE OF CONTENTS

ABSTRACT

The rate of iodine atom recombination in the presence of various gases has been studied by the flash photolysis technique. The temperature dependence of the rate constant has been determined for recombination in helium, hydrogen, benzene, and methyl iodide. The negative temperature dependences are fitted by the form, $k \propto 1/T^n$, where $n(He) = 0.80$, $n(H_2) = 1.48$, $n(C_6H_6) = 2.53$, and $n(CH_3I) = 3.24$.

The iodine atom recombination rate constant was also measured at 50°C. for ethyl iodide, hydrogen iodide, carbon monoxide, and nitric oxide. The rate constants relative to helium at 50°C. are:

He	1.00	C_2H_5I	179.
H_2	3.33	HI	21.1
C_6H_6	61.1	CO	4.07
CH_3I	88.8	NO	$>1.4 \times 10^4$

Nitric oxide appears to be a very efficient third body gas and only a lower limit on the rate constant could be established.

Calculations have been made for some possible mechanisms of iodine atom recombination. A classical three body collision model is proposed for atom recombinations. The classical equations of motion were programmed to be solved numerically on a digital computer and some trajectories were examined.

I. INTRODUCTION

The rate of the homogeneous gas phase iodine atom recombination in the presence of a third body atom or molecule has been studied by several methods. The early measurements of Rabinovitch and Wood(1) by a photostationary state method gave room temperature iodine recombination rate constants for several third body gases. Britton, Davidson, Gehman, and Schott(2) have used shock tube methods for recombination in argon, helium, oxygen, nitrogen, and carbon dioxide at high temperatures (1000-1600°K.). The flash photolysis technique has been applied by many investigators (3, 4, 5, 6, 7, 8, 9) to directly obtain the recombination rate in the 300-600°K. range.

Flash photolysis, as applied to kinetic measurements, consists of creating an unstable species in a system by a short, intense pulse of proper wavelength light. The light pulse should be of short duration compared to the rate of disappearance of the species and is usually obtained by discharging large condensers through a gas filled flash lamp. The concentration of the unstable species can be followed by its light absorption, recorded by a photodetector, and displayed on an oscilloscope screen. Such systems have been used to study unstable species with half lives as short as a few hundred

microseconds and even shorter. In iodine recombination rate measurements, a small fraction of the iodine is dissociated and the iodine atom concentration is followed indirectly by the visible absorption of iodine molecules.

The overall simple recombination reaction and rate equation are:

(1) $$I + I + M \xrightarrow{k(M,\ T)} I_2 + M$$

(2) $$-\frac{d[I]}{dt} = 2k(M,\ T)\ [I]^2\ [M]$$

where M is a third body atom or molecule. The third order rate constant at a given temperature, T, will be denoted by $k(M,\ T)$, where the temperature will be specified as either Centigrade or Kelvin degrees. The units of this rate constant will always be taken as liter^2 mole^{-2} seconds^{-1} in this thesis.

There are three generalizations which are evident from previous iodine recombination rate measurements. (a) The third order rate constant at a given temperature depends on the nature of the third body gas. The magnitude of the rate generally increases with the expected degree of interaction between the third body atom or molecule and an iodine atom. (b) The third order rate constant has a negative temperature dependence, the exact dependence varying with the third body. (c) Molecular iodine is itself a very efficient third body at lower temperatures and thus all observed rates

necessarily involve a contribution from $k(I_2, T)$. These generalizations are not in disagreement with the results presented here.

The extensive measurements of Russell and Simons (4) gave recombination rates for 29 different gases, which varied in magnitude from $k(He, 25^{\circ}C.) = 1.38 \times 10^{9}$ liters^{2} moles^{-2} sec.$^{-1}$ to $k(Mesitylene, 25^{\circ}C.) = 4.20 \times 10^{11}$ liters^{2} moles^{-2} sec.$^{-1}$. They found that a plot (figure 7) of "molecular association," as reflected by the normal boiling point of the third bodies, against rate constants, yields an approximately linear relationship. There were several exceptions, notably aromatic hydrocarbons, ethyl iodide, hydrogen, and helium. These exceptions are gases which would either exhibit greater than "inert gas" interactions with iodine atoms, or which might exhibit quantum mechanical effects. This thesis is generally concerned with the measurements of the rate constants for these exceptions.

The iodine recombination rate constants were measured in the presence of helium, hydrogen, benzene, methyl iodide, ethyl iodide, carbon monoxide, hydrogen iodide, and nitric oxide. The temperature dependence of the rate constant has been obtained for the first four gases.

II. THE EXPERIMENTAL APPARATUS

The apparatus used in this study was essentially that used by by Bunker (10), and the design will be described only briefly. Some modifications were made and the modified apparatus is shown in figure 1.

The gas cell, which contains the reaction mixture, is a pyrex cylinder 33 cm. long and 5 cm. in diameter, with a large side arm and U-tube connected as in figure 1. The U-tube contains a few grams of iodine crystals and is thermostated to obtain various vapor pressures of iodine in the gas cell. One branch of the side arm is heated electrically, so that the gas will circulate over the iodine and produce a homogeneous gas sample. The gas cell has flat pyrex windows on the ends and is connected to a conventional gas handling vacuum line.

A flash lamp is suspended above the gas cell, separated by a Corning #3486 glass filter. Light of longer wavelength than about 5000 Å. is passed by this filter, and causes dissociation into two normal $^2P_{3/2}$ iodine atoms. The pyrex flash lamp is about 36 cm. long and 13 mm. in diameter and is filled with 5 cm. of xenon after thorough degassing. The two electrodes are either conical or

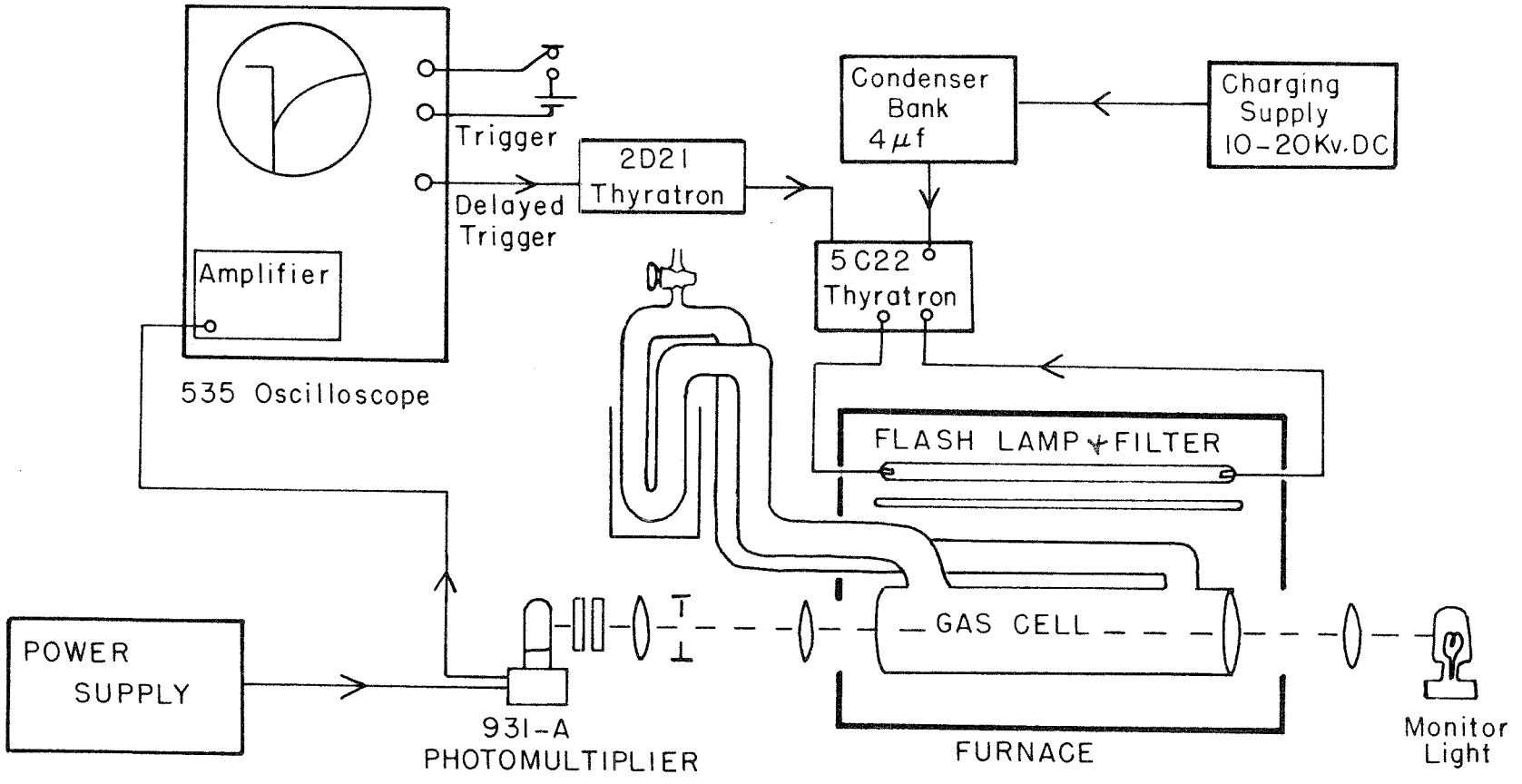

Figure 1
DIAGRAM OF APPARATUS

pointed nickel cylinders with tungsten leads and uranium glass seals.

The gas cell, filter, and flash lamp are all housed in an aluminum and asbestos furnace capable of regulated temperatures from ambient to about 275°C. The regulator system was replaced with a bimetallic element regulator system made by the American Instrument Company. A simple thermocouple and electrical bridge circuit are used to measure the furnace temperature. This regulator is generally sufficient to keep the temperature to within 2°C. of the desired temperature.

The monitor light source is a 500 watt tungsten projection bulb operating from a 120 volt battery bank. This light is focused through the gas cell, through two filters, and onto the photocathode of a 931-A photomultiplier tube. A Corning #3387 glass filter and a M-486 interference filter are used to select a wavelength band of approximately 100 Å. centered at 4860 Å. to be viewed by the photomultiplier. This is the continuum region of the I_2 absorption spectrum and is used to follow the I_2 concentration by the application of Beer's law. The specially designed photomultiplier circuit, featuring fast response and good linearity, has been described by Bunker (10). This circuit contains a precision Helipot potentiometer and a bucking battery so that the D.C. output may be set at zero. The Helipot reading is then proportional to the D.C. output of the photomultiplier.

A regulated power supply is used to provide a variable 40 to 70 volts per stage. The photomultiplier housing is shielded with enough metal to suppress most electrical interference due to the flash lamp discharge.

The photomultiplier output is connected to a Tektronix 53/54D D.C. differential amplifier which is a plug-in unit for a Tektronix 535 oscilloscope. A Dumont oscilloscope and associated amplifiers were used with the helium and hydrogen rate measurements as described by Bunker (10). The oscilloscope trace is photographed by a Polaroid camera. With the Tektronix oscilloscope it is possible to eliminate much of the trouble with external delaying circuits, and the electronics and cathode ray tube probably possess greater linearity.

The sweep of the Tektronix oscilloscope is triggered manually to give a base line from which to measure deflections. At a preselected point on the sweep, the oscilloscope generates a delayed trigger pulse which indirectly serves to initiate the discharge of the flash lamp. This 20 volt delayed trigger pulse causes a 2D21 thyratron to discharge and generate a 200 volt spike. The spike is applied to the control grid of a 5C22 high-current hydrogen thyratron and the resulting breakdown allows a 4μf condenser bank to discharge through the flash lamp. A high voltage power supply is used to charge the condenser bank to between 10 and 16 kilovolts, depending on the flash intensity desired. The hydrogen thyratron circuit and cables

to the flash lamp are designed to discharge the condenser bank in a minimum of time.

Before a typical experiment is started, the gas cell is filled with the desired pressure of the third body gas, and the electronics and monitor light are turned on. The U-tube containing the iodine is kept at a temperature somewhat less than that corresponding to the desired vapor pressure of iodine. The gas is circulated through the U-tube for 1/2 to 3 hours by means of the heater on one arm of the tube. After the optical density of the gas cell becomes and remains relatively constant, the heater is turned off and the actual run is started. The condenser bank is charged (in about 30 seconds), the Polaroid camera shutter is opened, and the measurement sequence is started by manually triggering the Tektronix oscilloscope sweep. Between 5 and 7 such recombinations are recorded over a period of about 10 to 15 minutes. Since there is some drift in the system and instruments, the D.C. level is measured and recorded between each recombination measurement. The conversion factor between Kelipot units and oscilloscope grid deflection units is also measured before and after a series of recombination measurements. At the end of a series, the cell is pumped out, a dry ice bath placed on the U-tube, and the new D.C. level measured so that the iodine concentration may be calculated. A scattered light and noise test is then made by discharging the flash lamp in the same sequence as for a recombination measurement.

III. DETAILS OF DATA INTERPRETATION

1. Kinetics of Recombination

For the idealized kinetic system resulting from the flash photolysis of iodine vapor in excess third body gas, M, the recombination reactions and rate equation are:

(3) $$I + I + M \xrightarrow{k_1} I_2 + M$$

(4) $$I + I + I_2 \xrightarrow{k_2} 2\,I_2$$

(5) $$I + I + I \xrightarrow{k_3} I_2 + I$$

(6) $$-\frac{d[I]}{dt} = 2k_1[I]^2[M] + 2k_2[I]^2[I_2] + 2k_3[I]^3$$

Conservation of iodine atoms requires the relationship:

(7) $$[I_2]_\infty = [I_2] + \frac{1}{2}[I]$$

where $[I_2]_\infty$ is the overall iodine molecule concentration and the non-subscripted concentrations are time dependent. The rate equation may now be exactly integrated between appropriate limits:

(8) $$\int_{[I]_o}^{[I]} \frac{d[I]'}{[I]'^2(a + b[I]')} = -\int_0^t dt'$$

$$t = \frac{1}{a}\left(\frac{1}{[I]} - \frac{1}{[I]_o}\right) - \frac{b}{a^2} \ln \left|\frac{(a + b[I])[I]_o}{(a + b[I]_o)[I]}\right| \qquad (9)$$

where $[I]_o$ is the initial iodine atom concentration and,

$$a = 2k_1[M] + 2k_2[I_2]_\infty \qquad b = 2k_3 - k_2 \quad .$$

If iodine atoms act as "inert gas" atoms, the last reaction (equation 5) might be expected to have a rate constant about twice that of the first reaction (equation 3) with M = Xe. There is no direct experimental evidence on k_3, since the concentration of iodine atoms is usually small. It has been found (10) that the observed recombination kinetics are independent of the initial iodine atom concentration, and this tends to exclude any relatively large value for k_3.

The second reaction (equation 4) becomes important when k_1 is small, since k_2 is quite large at lower temperatures. If the initial degree of dissociation is small, the I_2 concentration may be considered constant and included as part of the total third body concentration. This assumption has been used in analysing the experimental data. If k_3 is assumed negligible and $[I_2]_o \gg [I]_o$, equation 9 reduces to:

$$t = \frac{1}{2k_1[M] + 2k_2[I_2]_t}\left(\frac{1}{[I]_t} - \frac{1}{[I]_o}\right) \qquad (10)$$

since the ratio, b/a^2, will generally be quite small.

Equation 10 was used to analyze all kinetic data, although it is useful to consider the consequences of the full kinetic expression.

A plot of $1/[I]$ vs time yields a straight line according to third order kinetics (equation 10). The slope of the line is $1/(2k_1[M] + 2k_2[I_2])$ and the $t = 0$ intercept is inversely proportional to $[I]_o$.

The full kinetic expression (equation 9) predicts that the slope of a $1/[I]$ vs time plot will increase as time increases. This effect could be important for third body gases which have small rate constants, and could fulfill the condition, $k(M, T)[M] \leq k(I_2, T)[I_2]$.

Recombination in helium at 200 mm. and 50°C. was considered for "back calculation" of this "kinetic effect." The iodine molecule concentration was assumed to be 1.5×10^{-5} moles/liter with 10% initial dissociation. All the necessary rate constants were obtained from table 2. Figure 2 shows the calculated kinetic behavior of equation 9, plotted as time vs a dimensionless parameter, $\beta = [I]_o/[I]$. The maximum error in slope (or rate) is about +3.6%. For comparison, the "ideal" and "thermal effect" kinetic plots are also shown for helium with the same initial conditions. Since the conditions chosen represent the lowest temperature, lowest pressure, and highest $[I_2]$, this is the maximum kinetic effect expected. This effect is of decreasing importance for argon and hydrogen and is negligible for benzene and other more efficient third body gases.

2. Thermal Effect

Early flash photolysis measurements of iodine recombination rates (3, 4, 5) were made using more powerful flash lamps and lower

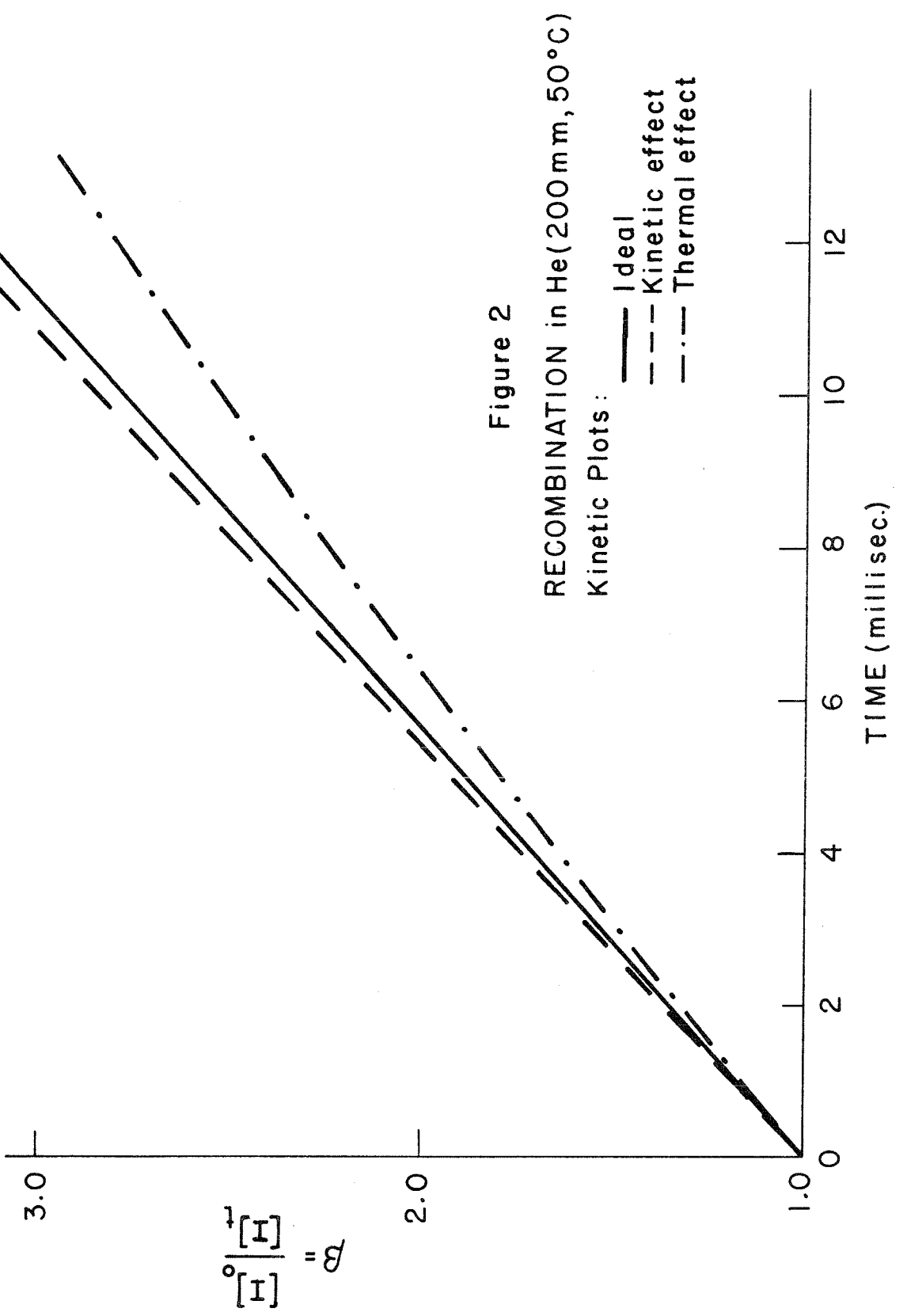

Figure 2

RECOMBINATION in He(200mm, 50°C)

gas pressures than are presently used. These caused more initial dissociation of iodine and excessive heating of the gas sample as the iodine atoms recombined. The magnitude of this heating depends on heat conduction to the walls, heat capacity of the gas, recombination rate, degree of dissociation, and other factors. Recombination rate measurements are made over periods of time comparable to the time for heat to diffuse from the gas to the cell walls. Since the outer layers of gas will cool faster than the more centrally located gas, the temperature distribution will not be uniform across the gas cell. The gas nearer the center of the cell will expand slightly and thus decrease the measured iodine molecule concentration. The calculated iodine atom concentration will then be too high, so that the observed rate will be lower than the actual rate for a given gas sample. Later flash photolysis measurements have generally avoided this thermal effect by using smaller initial degrees of dissociation, shorter flash durations, and higher gas pressures.

This thermal effect has been treated by Bunker and Davidson (9, 10) to give a conservative estimate of its importance. The working equations that were arrived at are:

(11) $$k_{apparent} = k_{actual}\,(1 - C)$$

(12) $$C = f(\beta) \cdot \left(\frac{4\pi b\, \phi}{r} \right) \cdot \left(\frac{D_1}{2^{\frac{1}{2}} k' [I]_o} \right)^{\frac{1}{2}}$$

(13) $$f(\beta) = \frac{\beta(5\beta - 4)}{4(\beta - 1)^{3/2}}$$

where, g = a small number between 1 and 3,

$h = \Delta H / C'T$, ΔH = heat liberated on recombination = 60 kcal/mole,

C' = average of C_v and C_p of third body gas,

r = radius of gas coil,

D_1 = heat diffusivity at one atmosphere,

P = pressure of third body gas,

$\beta = [I]_o / [I]$,

$k' = k(M, T)[M] + k(I_2, T)[I_2]_o$,

and $\phi = [I_2]_o / [M]$.

To evaluate these expressions for some of the third bodies used in this thesis, the extreme values of $[I_2]$ and $[M]$ were used so as to maximize the thermal effect. All necessary rate constants were obtained from table 2. Thermodynamic data was obtained, by interpolation when necessary, from the International Critical Tables (11), the National Bureau of Standards Tables (12), or from Hirschfelder, et al. (13). The quantities which did not change were taken as: $g = 2.5$, $r = 2.5$ cm., $[I_2]_\infty = 1.5 \times 10^{-5}$ moles/liter, and $[I]_o = 3 \times 10^{-6}$ moles/liter. The results of these calculations are found in table 1. Since β goes from 1.1 to about 3.0, $f(\beta)$ goes from 1.3 to about 5.8. The slope is generally measured where β is

Table 1

Calculated Parameters for Thermal Effect

Gas	Temperature	Pressure	D_1	$C/f(\beta)$	$\frac{k(\text{apparent})}{k(\text{actual})}$
Helium	50°C.	200 mm.Hg	1.95 $cm.^2/sec.$	0.047	0.939
"	275	200	3.61	.041	.947
Hydrogen	50	200	1.85	.028	.964
"	275	200	4.45	.026	.966
Benzene	50	50	0.10	.008	.987
"	200	50	0.35	.021	.973
Methyl iodide	50	50	0.058	.009	.988
"	200	50	0.136	.017	.978

about 1.1 and this fact is used to calculate the ratio, $k_{apparent}/k_{actual}$.

Helium and hydrogen give errors of about -6% and about -3-1/2%, respectively, depending slightly on the temperature. The actual pressures of helium or hydrogen were usually several fold greater than 200 mm. and the iodine concentration usually less than 1.5×10^{-5} moles/liter. These percentages are thus the upper limits and the actual error due to thermal effect is probably less than -2%. For benzene and methyl iodide the upper limit of error is less than -3% and the actual error is probably much less. The reason for the increase in thermal effect with temperature is due to the relatively large negative temperature dependence of the rate for benzene and methyl iodide.

Figure 2 gives an approximate kinetic plot for helium (200 mm., 50°C.) with the thermal effect included. The actual kinetic plots of experimental data for helium and hydrogen generally showed a slight upward curve, as if a slight kinetic effect is present without much thermal effect. Experimental measurements of iodine atom concentration after $\beta > 2$ are subject to considerable error, and it is difficult to draw conclusions as to the cause of this curving. The kinetic plots for benzene and methyl iodide generally followed the "ideal" straight line.

It is also interesting to note that the kinetic effect is also

largest under the same extremes in initial conditions, but it causes an increased rate constant. Thus the two effects generally tend to partially cancel each other.

3. Errors

The sources of errors associated with these measurements have been discussed previously (10). Some random errors contributing to the spread of the observed rate constants are noise, error in measurement of scaling factors, initial degree of dissociation, errors in measurement of deflections, and gas temperature. The effect of random error can be reduced by averaging the results of a large number of measurements. Some possible systematic errors are the thermal effect, the kinetic effect, errors in concentration measurement, and nonlinearity in the electronics, the photomultiplier tube, and the cathode ray tube.

The use of a Tectronix 535 oscilloscope in all measurements except helium and hydrogen may have resulted in less noise and better linearity in the electronics and cathode ray tube. Since this oscilloscope has accurately timed sweep rates, it was also possible to eliminate the error in the measurement of a time scale factor.

4. Calculation of Observed Rate Constants

A typical recombination trace photograph is sketched in figure 3. A base line, A, is initially obtained and its distance from D.C. zero is denoted by y_o. The location of D.C. zero is greatly

exaggerated in figure 3 and would actually be several feet below this figure.

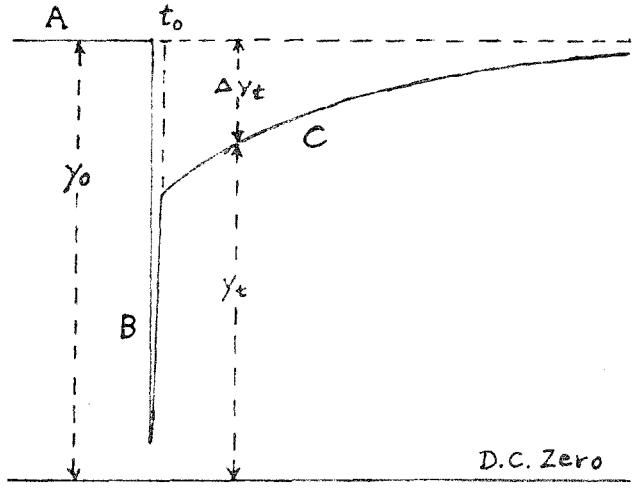

Figure 3

Immediately after the thyratrons are triggered, the flash lamp fires and causes a spike, B, due to scattered light entering the photomultiplier. Starting at time t_o, the actual recombination trace, C, is observed. The total deflection at time t is called y_t, and the quantity, $\Delta y_t = y_o - y_t$, is measured at about 10 different times. The actual position of t_o (usually about 200 microseconds after flash) is located by comparison with empty gas cell flash experiments. With the gas cell empty, the base line to D.C. zero distance is also measured and denoted as a. Since y_o and a are measured in Helipot units and Δy_t in grid units of the scope screen, it is necessary to have a scale conversion factor, F. The proper time scale was known by the sweep rate of the Tektronix 535 oscilloscope.

In terms of the deflections already defined, the iodine atom and molecule concentrations are given by:

$$[I]_t = \frac{2}{\epsilon L} \log_{10} \left(\frac{y_o - \Delta y_t}{y_o} \right) \tag{14}$$

$$[I_2]_t = \frac{1}{\epsilon L} \log_{10} \left(\frac{a}{y_o} \right) \tag{15}$$

where ϵ is the decadic extinction coefficient and L is the cell length in centimeters. The measurements of Bunker (10) were used for values of ϵ for iodine. The third body concentration was calculated by assuming it to be an ideal gas.

If equation 2 is integrated between the appropriate limits, the third order kinetic equation is:

$$2 k_{obs.}(M, T) [M] (t - t_o) = \left(\frac{1}{[I]_t} - \frac{1}{[I]_o} \right) \tag{16}$$

where $k_{obs.}(M, T)$ is the observed rate constant for the total third body concentration in the gas sample. The calculated values of $1/[I]_t$ are plotted against t and yield a straight or slightly curving line. From the slope of this line, the observed rate constant can be found. From the intercept of this line at "flash discharge time," the initial iodine atom concentration may be calculated and usually corresponds to about 10% dissociation. The actual kinetic plots are often slightly curved "upward" due to the kinetic effect and error in measuring small deflections. The slope of the kinetic plot was usually taken

near t_o to minimize the effects of this curving.

A program for the Electrodata 205 digital computer was written to reduce the experimental data to kinetic information. This program would least square the calculated values of $1/[I]_t$ vs t and use the results to calculate $k_{obs.}$ (M, T), $[I_2]_o/[M]$, and their probable errors. $[I_2]_o$ is the iodine molecule concentration corrected for the amount of dissociation at t_o. This program was able to relieve some of the tedium associated with data reduction. Its main drawback was occasional erroneous results due to the lack of judgment by the computer in rejecting obviously faulty data points.

For each gas sample there were obtained 5 to 7 acceptable rate measurements which were averaged. These average rates (for a given gas and temperature) were plotted against their corresponding $[I_2]_o/[M]$. The points of this plot were fitted to a straight line by a least squaring program written for the Electrodata computer. The slope and intercept of this line were calculated along with the probable errors in each. Since there are always iodine molecules present, the observed rate must be corrected for the high efficiency of iodine molecules in recombination. The intercept (at $[I_2]_o/[M] = 0$) is then k(M, T) for the given third body gas. The slope of this line is $k(I_2, T)$. The calculated $k(I_2, T)$ should be the same for all third body gases at a given temperature, although it is subject to considerable experimental error, particularly at higher temperatures.

IV. RESULTS

1. Argon

A few runs were made with argon as third body to check the technique and to compare with the argon results of Bunker and Davidson (9) which were obtained on essentially the same apparatus. Linde argon (99.99%) was used after passage through a dry ice trap. The average values obtained (two runs each) were $k(A,\ 50^{\circ}C.) = 3.15 \times 10^9$ and $k(A,\ 150^{\circ}C.) = 1.84 \times 10^9$. These compare well with the values of $(2.99 \pm 0.13) \times 10^9$ and $(1.66 \pm 0.05) \times 10^9$, respectively, previously obtained by Bunker and Davidson.

All rates reported in this section, unless otherwise stated, are the results of least squaring by digital computer (of $[I_2]_0/[M]$ vs $k_{obs.}(M,\ T)$) or of averaging the corrected rates. All stated limits of error are probable errors and all rates are in units of $liters^2\ moles^{-2}\ seconds^{-1}$. A complete list of rates and their probable errors is given in table 2.

2. Helium

Measurements of the recombination rates of iodine atoms with helium as third body were made at 30, 150, and 275°C. Ohio Chemical Company helium was passed through a liquid nitrogen or dry ice

Table 2

Gas	Runs	T°C.	$k(M, T) \times 10^{-2}$	$k(H_2, T) \times 10^{-11}$
A	2	50	3.15 ± .0	12.0 ± .0
	2	150	1.84 ± .0	1.90 ± .0
He	15	50	1.33 ± 0.06	9.73 ± 1.0
	5	150	1.64 ± 0.03	2.27 ± 0.53
	3	275	0.87 ± 0.10	1.23*
H_2	6	150	2.84 ± 0.10	2.27**
	2	275	2.03 ± 0.13	1.23*
C_6H_6	3	50	81.2 ± 4.4	10.7*
	3	100	57.2 ± 3.8	4.42*
	3	200	31.0 ± 1.3	0.96*
CH_3I	3	50	118. ± 5.	10.7*
	3	100	69.7 ± 2.9	4.42*
	3	200	34.0 ± 2.1	0.96*
C_2H_5I	2	50	238. ± 23.	10.7*
CO	2	50	5.42 ± 0.16	10.7*
HI	3	50	28.1 ± 1.8	10.7*
NO	3	50	$> 1.8 \times 10^4$	. . . .
	1	200	. . . . .	. . . .

All rates are in liters^2 moles^{-2} seconds^{-1}.

"Runs" are the number of runs included in averages.

*Assumed values from Bunker's argon data.

**Assumed values from the helium data.

bath before use. Plots of the average observed rate constant vs $[I_2]_o/[He]$ for each run are shown in figure 4 along with the least squares straight line.

At 50°C., as much as half of the observed rate can be due to $k(I_2, 50°C.)$, and this may account for some of the scatter in points, since the observed rate will be sensitive to error in iodine concentration as well as error in gas sample temperature. The kinetic and thermal effects can also cause error in low temperature helium measurements. The slope of the least squares fit gives $k(I_2, 50°C.) = (9.73 \pm 1.0) \times 10^{11}$ which compares favorably with $(1.07 \pm 0.16) \times 10^{12}$ obtained by Bunker and Davidson (9) with argon. The intercept value of $k(He, 50°C.) = (1.33 \pm 0.06) \times 10^9$ is probably better than the probable error in $k(I_2, 50°C.)$ would indicate, since most of the data points lie relatively close to the intercept.

A least squares fit gave $k(I_2, 150°C.) = (2.27 \pm 0.53) \times 10^{11}$ which compares with Bunker and Davidson's value (9) of $(1.43 \pm 0.38) \times 10^{11}$ from argon measurements. The possible errors in $k(He, 150°C.) = (1.04 \pm 0.03) \times 10^9$ could be due to thermal effect.

At 275°C., only three of the four helium runs yielded reasonable rates. Due to the small contribution of $k(I_2, 275°C.)$, Bunker and Davidson's value of $k(I_2, 275°C.) = 1.23 \times 10^{11}$ from argon measurements was used to correct the observed rates.

Figure 4

k(M,T) vs. $[I_2]/[M]$

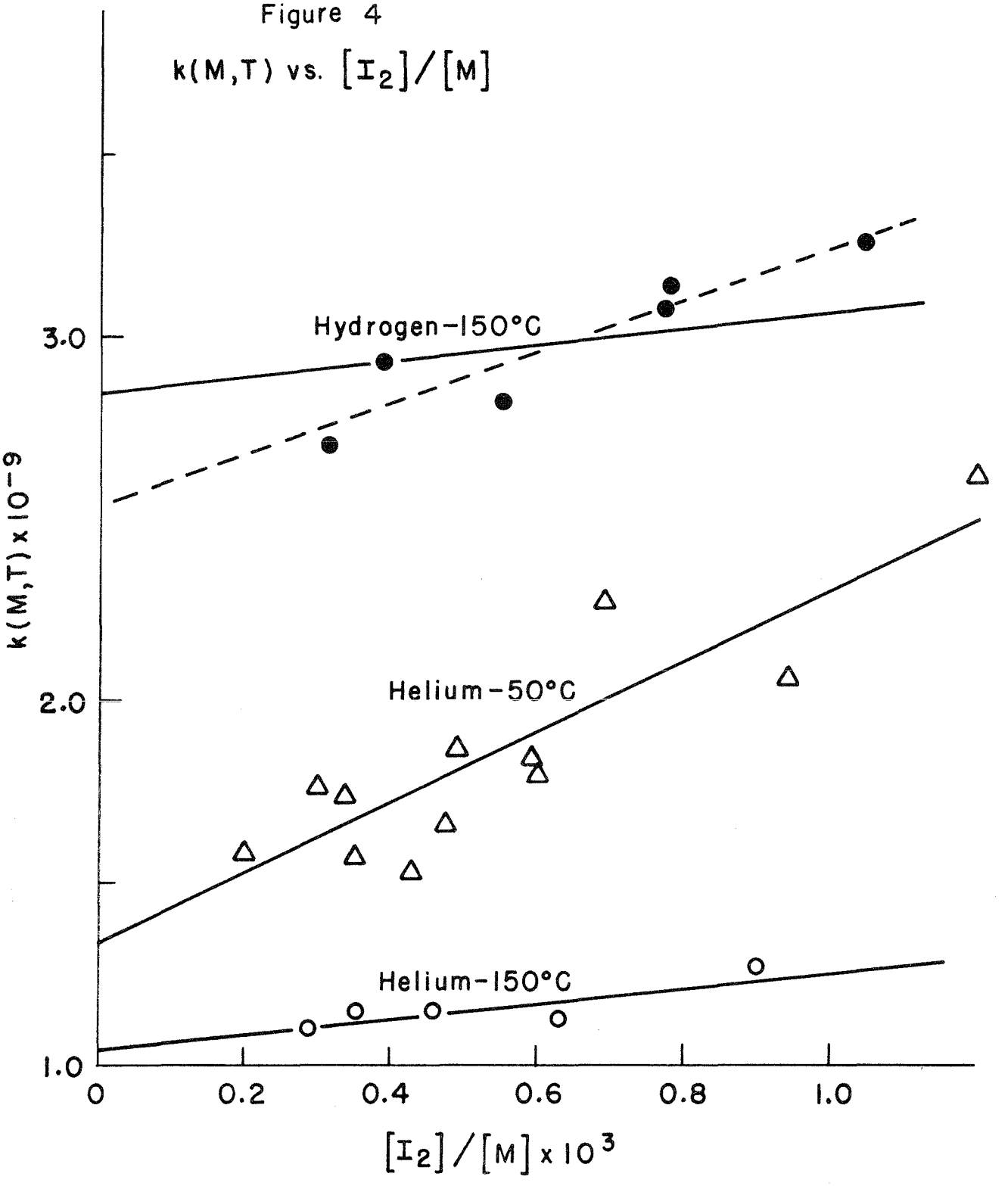

Two convenient forms for fitting the temperature dependence of these rate constants are $1/T^n$ and $e^{E/RT}$. The rate constants have been plotted in figure 5 as $\log_{10}k(M, T)$ vs $\log_{10}T$ and in figure 6 as $\log_{10}k(M, T)$ vs $1/T$. The least square straight lines are also shown. From the slope and intercept of this line, the two constants in the assumed temperature dependence can be calculated.

For helium, the temperature dependence obtained was:

(17) $$k(He, T^\circ K.) = 1.41 \times 10^9 (298/T)^{0.80 \pm .04}$$

(18) $$k(He, T^\circ K.) = 10^{(4.09 \pm .03)} \exp(0.662 \pm .003 \text{ kcal}/RT)$$

Britton, et al. (2) have measured iodine dissociation rates in helium and other gases at high temperatures using shock tube methods. Using their value of $k(He, 1400^\circ K.) = 1.8 \times 10^8$ and the value of $k(He, 50^\circ K.) = 1.33 \times 10^9$ obtained here, the temperature dependence is fitted by: $k(He, T^\circ K.) = 1.48 \times 10^9 (298/T)^{1.36}$. If equation 17 is extrapolated to high temperatures, $k(He, 1400^\circ K.) = 2.6 \times 10^8$, which compares well with the shock tube value.

Russell and Simons (4) measured recombination rates in helium and other gases at 20 and 127°C. Their work was done before the high efficiency of I_2 was realised and their rates have been roughly corrected for I_2 before presenting them here. These "corrected Russell and Simons" rates will hereafter be called "CRS" rates. For convenience of comparison, the present rates have been

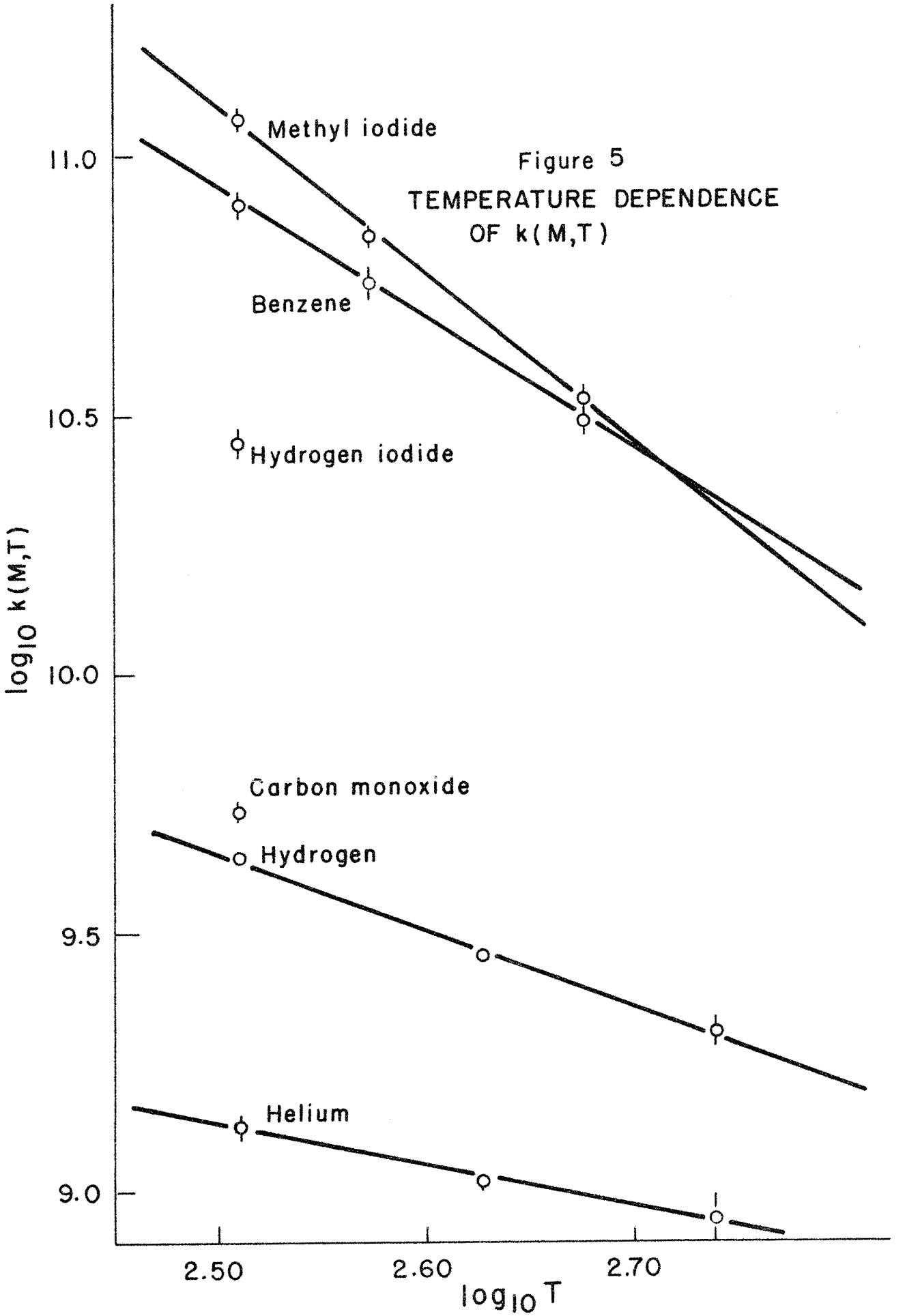

Figure 5
TEMPERATURE DEPENDENCE
OF k(M,T)

Figure 6
TEMPERATURE DEPENDENCE
OF k(M,T)

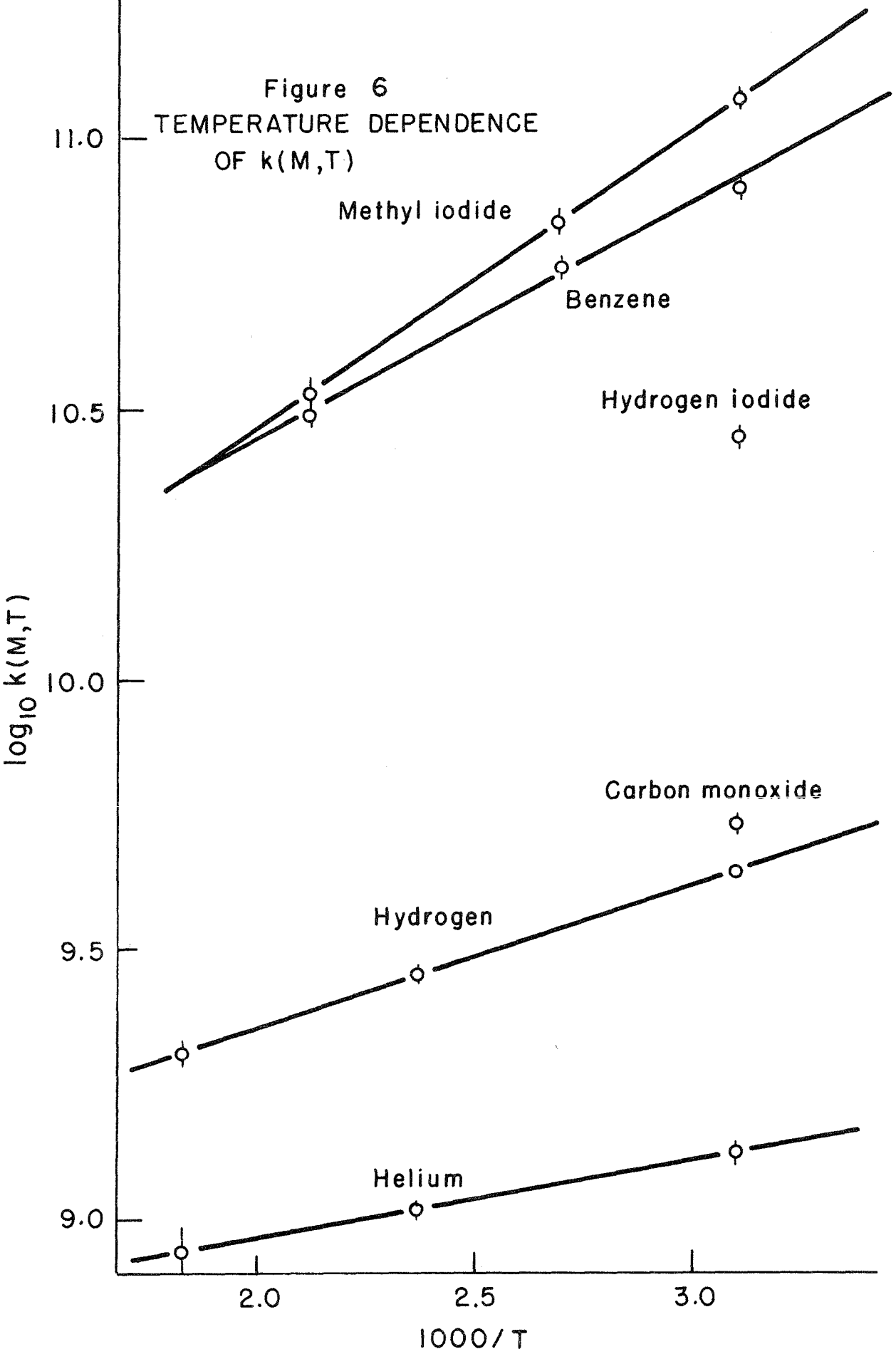

extrapolated to 20 or 127°C. using the experimental $1/T^m$ dependance. The CRS rates for helium are k(He, 20°C.) = 1.38×10^9 and k(He, 127°C.) = 0.82×10^9, compared to 1.47×10^9 and 1.08×10^9 for the respective rates from this thesis. The reason for the greater temperature dependence found by Russell and Simons is not known, although it is thought that thermal effects are less in the present set of experiments.

3. Hydrogen

Hydrogen was taken from a Linde cylinder (99.9%) and was passed through a dry ice trap before filling the gas cell. Measurements were made at 150 and 275°C., since Bunker and Davidson (9) obtained good results with hydrogen at 50°C. on the same apparatus.

A least squares fit of the 150°C. runs (figure 4, dashed line) gave k(H_2, 150°C.) = $(2.54 \pm .07) \times 10^9$ and k(I_2, 150°C.) = $(7.06 \pm .99) \times 10^{11}$. This k($I_2$, 150°C.) is five times greater than Bunker's argon-derived rate and three times greater than the helium-derived rate found here. If the observed rates are corrected for k(I_2, 150°C.) from the helium measurements, and the corrected rates averaged, there results: k(H_2, 150°C.) = $(2.84 \pm .10) \times 10^9$ (figure 4, solid line). This last value is considered more reliable, although the limits of probable error should be considerably larger.

It seems possible that thermal effect or thermal and photochemical formation of hydrogen iodide may be causing some systematic error. The rate of homogeneous thermal formation can be

shown to be quite small (Appendix I), but the contributions of heterogeneous and photochemical reactions are not known. If the dissociating flashes were producing hydrogen iodide, the rates would tend to increase during a run, but this was not observed. No correlation was found between the average observed rates of runs with long or short heating and irradiation (with monitor light) times. An infrared spectrum of a gas sample which had been heated and illuminated for four hours showed no absorption at 4.33 μ (fundamental vibrational frequency of HI). The influence of hydrogen iodide cannot be completely settled from this evidence, since only 1% conversion of the hydrogen will result in about 10% change in observed rate.

Unfortunately, only two of the hydrogen runs at 275°C. were considered successful. These rates were corrected for $k(I_2, 275^{\circ}C.)$ and the rates averaged. The least squares fit (figures 5 and 6) of the temperature dependence plot gave:

(19) $$k(H_2, T^{\circ}K.) = 4.93 \times 10^9 (298/T)^{1.48 \pm .07}$$

(20) $$k(H_2, T^{\circ}K.) = 10^{(8.82 \pm .01)} \exp(1.22 \pm .01 \text{ kcal}/RT)$$

By extrapolation, using equation 19, it was possible to obtain $k(H_2, 25^{\circ}C.) = 5.00 \times 10^9$. The CRS rate for the same conditions is 4.45×10^9.

4. Benzene

Reagent grade Baker and Adamson benzene was used (after degassing by freezing and pumping) in measurements at 50, 100, and 200°C. Since the contribution by iodine molecules to the observed rate is small for benzene (about 5% at 50°C.), the observed rates were corrected by using Bunker's $k(I_2, T)$ as derived from argon measurements. The resulting values of $k(C_6H_6, T)$ were averaged and the probable error found.

Due to the thermal effect and the vapor pressure of benzene, the pressure range was only 50 to 70 mm. of benzene. Three runs were pressurized with about 150 mm. of argon to check for the presence of thermal effect. The argon-benzene runs gave the same average rates as the benzene alone runs, after correction was made for the contribution to the rate by the added argon.

The temperature dependence (figures 5 and 6) was found to be:

(21) $$k(C_6H_6, T°K.) = 1.00 \times 10^{11} (298/T)^{2.53 \pm .07}$$

(22) $$k(C_6H_6, T°K.) = 10^{(9.59 \pm .05)} \exp(1.97 \pm .09 \text{ kcal}/RT)$$

Equation 21 may be used to extrapolate the rate to lower temperatures. This gives $k(C_6H_6, 20°C.) = 104 \times 10^9$ and $k(C_6H_6, 127°C.) = 47.5 \times 10^9$, to compare with the corresponding CRS rates of 86×10^9 and 27×10^9. The reason for the differences is not known.

although some thermal effect could be present in the CRS rates.

5. Methyl Iodide

A freshly opened bottle of Matheson C.P. grade methyl iodide was degassed by pumping and freezing and was stored in the dark over a piece of copper wire. The methyl iodide remained almost colorless throughout the experiments. The pressure range was 75 to 225 mm. of methyl iodide, and a pressurized run with 150 mm. of argon did not differ significantly when corrected for the added argon.

As with benzene, the observed rates were corrected for $k(I_2, T)$, and the rates averaged for each temperature (50, 100, and 200°C.). The temperature dependence plots yield:

(23) $$k(CH_3I, T°K.) = 1.50 \times 10^{11} (298/T)^{3.24 \pm .11}$$

(24) $$k(CH_3I, T°K.) = 10^{(9.37 \pm .01)} \exp(2.55 \pm .01 \text{ kcal}/RT)$$

The possibility of thermal or photochemical decomposition of methyl iodide at the higher temperatures was considered, but the measured rates of decomposition seem to be too small to affect the results obtained here. This seems to be the first measurement with methyl iodide, although Russell and Simons (4) have studied the ethyl halides at a single temperature.

6. Ethyl Iodide

A freshly opened bottle of reagent grade ethyl iodide was treated and stored as was methyl iodide. It remained slightly yellow during the experiments. Only two runs were made at 50°C. and the observed rates corrected for k(I_2, 50°C.). Both runs were with about 65 mm. of ethyl iodide, but one was pressurized with about 200 mm. of argon. The average corrected rates were within 10% of each other.

Assuming that this rate varies approximately as $1/T^3$, the extrapolated value is k(C_2H_5I, 25°C.) = 302×10^9. The CRC value is 251×10^9. Although not affecting the 50°C. measurement, extension of this measurement to high temperatures might have difficulties with thermal decomposition.

7. Carbon Monoxide

Matheson C.P. grade carbon monoxide was used directly in two runs to measure the recombination rate at 50°C. Correction of the observed rates for k(I_2, 50°C.) was made and the results averaged.

8. Hydrogen Iodide

Hydrogen iodide was prepared by the method suggested in Henderson and Fernelius (14). A slight excess (over the calculated stoichiometric quantity) of red phosphorous was mixed with iodine crystals and some clean dry sand in a flask. The air-tight system was flushed with argon at atmospheric pressure and then distilled

water slowly added to the mixture. The reaction was moderated with a wet towel placed on the outside of the flask. The liberated hydrogen iodide was passed through an ice-cooled trap filled with pyrex wool to remove some water and iodine vapor. It was collected in a liquid nitrogen trap after passing through a drying tube containing phosphorous pentoxide on glass beads. The hydrogen iodide obtained was dark colored, but two bulb to bulb distillations afforded a light yellow solid. This was stored in a dry ice trap in the dark and it did not discolor during the several days of experiment.

Three good runs were made with hydrogen iodide at 50°C. and pressures of 65, 118, and 220 mm. Some uncertainty was encountered in measuring gas pressures, since hydrogen iodide rapidly attracts mercury and the colored mercuric iodide tends to obscure the mercury manometer level. One run was made with no mercury in the system and the pressure was determined by the known vapor pressure of hydrogen iodide at dry ice temperatures (-78.5°C. is 65 mm. of HI). The observed rates were corrected for $k(I_2, 50°C.)$ and the resulting average rates had a spread of less than 10% between the three runs.

Hydrogen iodide will decompose during an experiment, but at 50°C., the homogeneous thermal decomposition is not fast enough to cause error (Appendix I). If extensive decomposition had occurred, there should be a decrease in pressure during the run, but

this was not observed. Since hydrogen is about one-sixth as efficient as hydrogen iodide, 1% decomposition will change the observed rate by only about 1%. It seems safe to conclude that the average corrected rate is valid.

9. Nitric Oxide

Matheson nitric oxide was purified by the method described by Huffman (15). Condensed nitric oxide was twice distilled from a methylpentane bath at -150°C. to a liquid nitrogen bath. This process changed the nitric oxide from a multicolored solid to a very light blue liquid or a light blue ice-like solid. This solid was stored in a liquid nitrogen bath.

To fill the gas cell, the vacuum line and cell were filled with atmospheric pressure argon and then re-evacuated. This was followed by the same treatment with 20 mm. of nitric oxide. Then the cell was filled with the desired pressure of nitric oxide and argon. This procedure was an attempt to eliminate free oxygen or colored nitrogen dioxide.

Table 3

Run #	Temperature	Nitric oxide	Argon
1	50°C.	442. mm.	none
2	50	27. mm.	146 mm.
3	50	v.p. at -78°C.	110 mm.
4	200	26. mm.	122 mm.

Only four runs were completed with nitric oxide and are given in table 3. Runs #2, 3, and 4 showed the same behavior. The oscilloscope trace of the recombination appeared to be essentially identical with the trace of scattered light with an evacuated gas cell. The behavior of run #1 was similar, except the recombination trace rose to just below the base line and then decayed very slowly to the base line. Run #1 was made with a less purified nitric oxide and presumably this behavior can be explained by recombination of oxygen atoms with nitric oxide to form the light absorbing nitrogen dioxide.

There are several ways of interpreting these results, but a simple third order recombination shall be assumed here. The typical flash duration is about 200 microseconds and it will be assumed that at that time, at least 19/20ths of the iodine atoms have disappeared. The assumed concentrations are $[I]_o = 2 \times 10^{-6}$ moles/liter and $[NO] = 1.3 \times 10^{-3}$ moles/liter. Substituting into the rate expression:

$$(25) \qquad k(NO,\ 50^{\circ}C.) = \frac{1}{2\,t\,[NO]^2}\left(\frac{1}{[I]} - \frac{1}{[I]_o}\right) \gtrsim 1.8 \times 10^{13}$$

This large rate is a lower limit and about ten times as large as $k(I_2,\ 50^{\circ}C.)$.

V. DISCUSSION

1. Introduction

The general theory of the gas phase iodine atom recombination was discussed by Wigner (16), Rabinowitch (17), Rice (18), and others in the late 1930's. The more recent contributions (19, 20, 21) have generally expanded the earlier arguments in light of the experimental developments and have elaborated on the actual calculations involved. These theoretical approaches have generally considered one of the possible limiting mechanisms for the overall reaction (equation 1). If the third body, M, is idealized as a hard sphere without any interaction with an iodine atom, the recombination can proceed by the "deactivation" mechanism,

(26) $$I + I \underset{}{\overset{K}{\rightleftharpoons}} I_2^*$$

(27) $$I_2^* + M \underset{}{\overset{PZ}{\rightleftharpoons}} I_2 + M$$

where I_2^* is a collision complex of very short lifetime. This mechanism has recently been examined by Bunker (20) and Kock (21).

The alternate "intermediate complex" mechanism can contribute if there is an interaction between the third body and the iodine

atom;

(28) $$I + M + M \underset{}{\overset{K}{\rightleftharpoons}} IM + M$$

(29) $$IM + I \xrightarrow{PZ} I_2 + M$$

where IM is the intermediate complex. It is possible to consider the IM as contributing to the second step only if it is in a bound state of the weak van der Waals potential. Alternately, it is possible to consider all IM complexes as contributing to the second step. Both these cases have been treated by Bunker and Davidson (19) and agreement is obtained with only the former hypothesis.

2. Intermediate Complex Theory

Before a comparison of this theory with experiment, a brief description of the Bunker and Davidson method (19) will be given. The first step, complex formation (equation 28), is a three body reaction, but is considered faster than the direct three body recombination, since there is always a large excess of third bodies present. The first step is assumed to always be in equilibrium with respect to those intermediate complexes which are in bound states of a Lennard Jones potential. The rate of the second step (equation 29) is taken as the product of a steric factor, P, and a collision number, Z. Then the recombination rate is $k(M, T) = PZK$, where K is the equilibrium constant for the first step.

The equilibrium constant is developed in terms of the classical partition functions. The only difficulty is in the evaluation of the internal partition function for the IM complex. It is assumed that the total internal energy must be less than the "dissociation energy" for the I and M to be considered as a complex and thus contribute to the second step. The IM interaction was assumed to be a Lennard Jones potential. For weak interactions they have derived an approximate expression for the equilibrium constant

$$K/\sigma^3 = \pi^{1/2} \left(\frac{\epsilon_o}{kT}\right)^{3/2} \left(\frac{8}{3} + \frac{32\,\epsilon_o}{45\,kT}\right) \tag{30}$$

where ϵ_o is the depth of the Lennard Jones potential and σ is the IM collision diameter. If the steric factor is temperature independent and the collision number varies as the usual $T^{1/2}$, the recombination rate will vary as approximately $1/T$ to $1/T^2$. This also shows that the third bodies with greater rates will also possess a greater negative temperature dependence.

Stogryn and Hirschfelder (22) have treated the classical equilibrium constant problem in greater detail. They have calculated the contribution of metastable intermediate complex to the equilibrium constant. Metastable complexes have an internal energy greater than the dissociation energy, but are prevented from dissociating by the angular momentum barrier. The contribution of metastable complexes to the equilibrium constant is considerably

smaller than the contribution of the bound complexes, but the equilibrium constants used here have been corrected for the metastable complex contribution.

The intermediate complex theory was used to calculate the recombination rates for various third bodies. The Lennard Jones parameters, ϵ_o and σ, were obtained from Hirschfelder, et al.(13). Potential parameters obtained from second virial coefficient data were used in preference to those obtained from gas viscosities. No parameters for methyl and ethyl iodides could be found in the literature, so very rough estimates were made (table 4). Iodine atoms were assumed to have the same ϵ_o and σ as xenon atoms, and the usual combining rules were used to obtain "mixed" potential parameters.

(31) $$\epsilon_{IM} = |\epsilon_I \cdot \epsilon_M|^{1/2} \qquad \sigma_{IM} = |\sigma_I + \sigma_M|/2$$

Collision numbers for the second step were calculated using the reduced mass of IM and I, and considering the collision radius of IM to be the larger value of either σ_I or σ_M. The steric factor was taken as one-half. An exception is the iodine molecule third body with a steric factor of unity, since either direction of collision should yield the same products. The possibility of an electronic steric factor will be neglected here, but will be mentioned later. Table 4 lists the intermediate values and the final calculated

Table 4

Gas	Temperature	ϵ_{IM}	σ_{IM}	kT/σ^3	k(calc.)*	k(exp.)*
He	50°C.	36.5°K.	3.365Å.	0.21	0.41	1.33
"	150	"	"	0.14	0.31	1.04
"	275	"	"	.09	0.23	0.87
H_2	50	80.4	3.485	.74	1.61	4.43
"	150	"	"	.49	1.21	2.84
"	275	"	"	.33	0.93	2.03
A	50	164.	3.750	2.50	6.40	2.99
"	150	"	"	1.58	4.62	1.66
"	275	"	"	1.00	3.32	1.13
Ne	50	88.7	3.425	0.87	1.75	1.36
Kr	50	194.	3.850	2.65	7.06	3.78
Xe	50	221.	4.100	4.50	13.8	3.98
N_2	50	146.	3.905	2.00	5.92	2.80
CO	50	149.	3.931	2.12	6.34	5.42
NO	50	170.	3.635	2.60	6.15	18000.
C_6H_6	50	312.	4.735	8.50	69.8	81.2
"	100	"	"	6.15	54.5	57.2
"	200	"	"	3.95	39.2	31.0
HI	50	268.	4.111	6.10	19.3	28.1
CH_3I	50	421.**	4.20**	14.0	50.8	118.
"	100	"	"	11.0	42.8	69.7
"	200	"	"	6.90	30.4	34.0
C_2H_5I	50	446.**	4.35**	15.5	71.4	238.
n-C_4H_{10}	50	256.	4.535	5.50	36.2	29.8
I_2	150	348.	4.541	6.00	81.0	143.
"	275	"	"	3.67	56.2	123.

*All k's given in liter^{2}moles^{-2}seconds^{-1} x 10^9.
**Estimated values.

and experimental rates. With the exception of nitric oxide, agreement within a factor of four is obtained.

Some of these calculated rates have been plotted against the experimental rates (figure 8). The dashed line represents the points for which, k(experimental)/k(calc.) = 1. Helium and hydrogen are considerably below this dashed line and thus the experimental rates are much greater than calculated. The negative temperature dependence of the hydrogen rates is underestimated by this calculation, which is reflected in figure 8 by the slope of the hydrogen points being less than the slope of the dashed line. This is true for all measured rates, with the exception of helium.

Benzene and the iodides are generally below the dashed line, probably due to stronger than van der Waals forces between them and iodine atoms. They also show much greater than calculated negative temperature dependence. The heavier rare gases (and simple molecules such as nitrogen) can generally be accounted for by decreasing the steric factor to about 1/4.

The assumption that classical statistical mechanics is sufficient for the calculation of equilibrium constants can be questioned in cases where the van der Waals forces are very weak. The complexes formed between a light gas, such as hydrogen or helium, and a halogen atom have only a few bound vibrational energy levels. Appendix II gives a detailed calculation of the vibrational energy

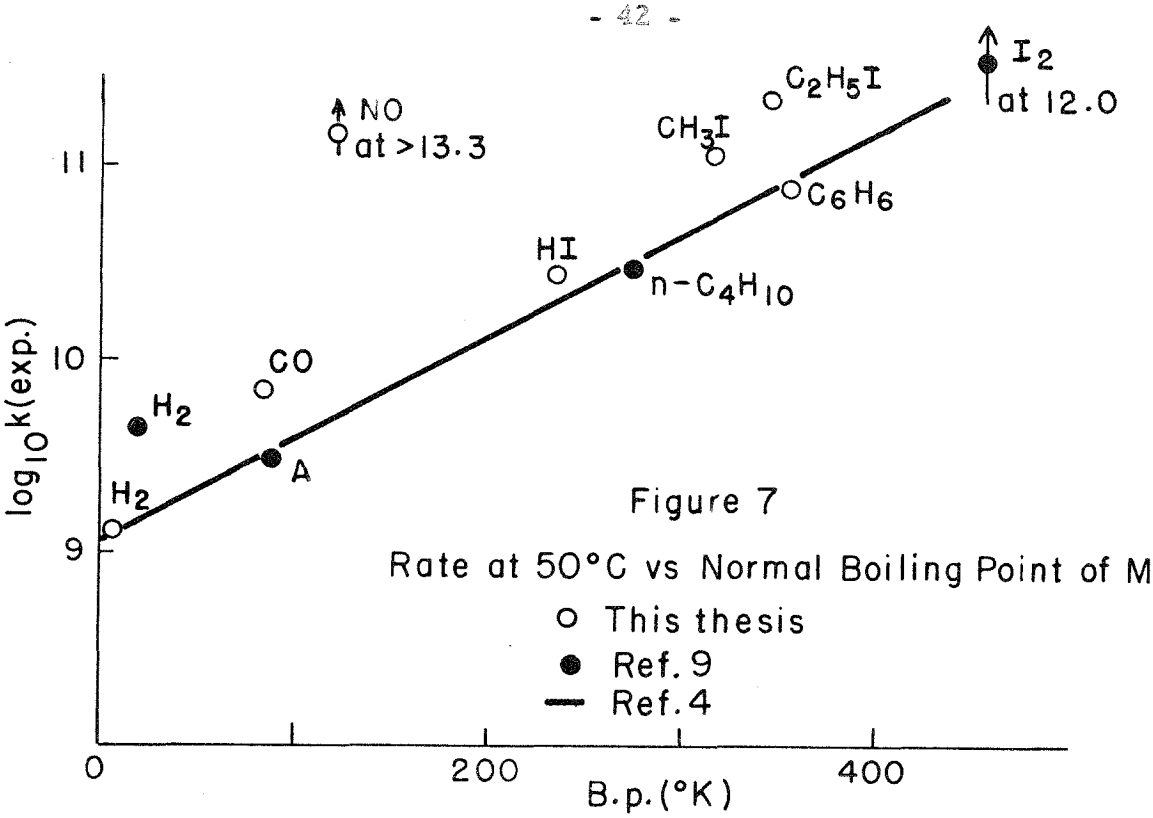

Figure 7

Rate at 50°C vs Normal Boiling Point of M

○ This thesis

● Ref. 9

— Ref. 4

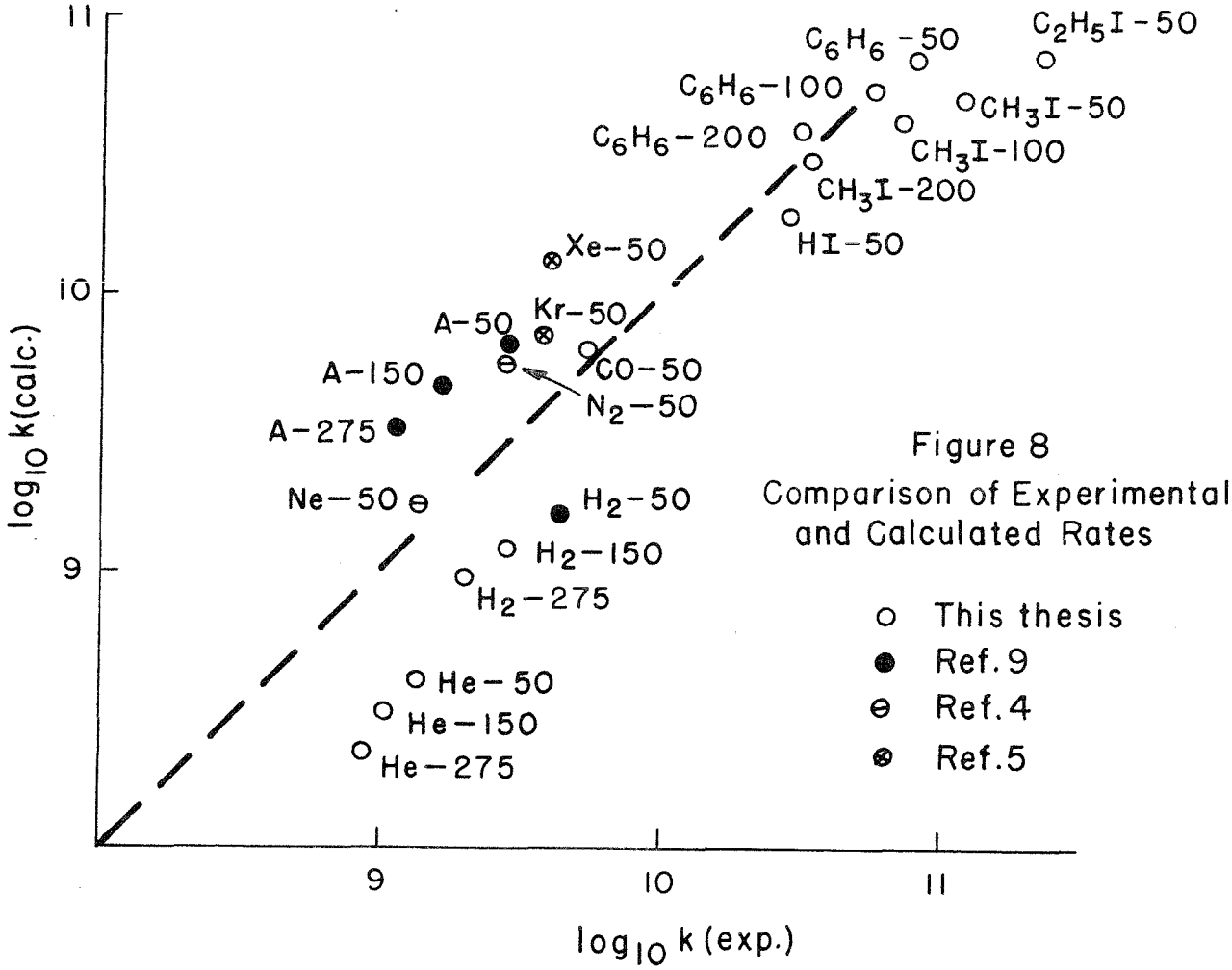

Figure 8

Comparison of Experimental and Calculated Rates

○ This thesis

● Ref. 9

⊖ Ref. 4

⊗ Ref. 5

levels for the Lennard Jones and several other potentials in terms of the dimensionless parameter, K. The general effect of the quantum statistics is to reduce the equilibrium constant, and thus lower the calculated halogen recombination rates. Appendix III shows this effect to be negligible for the halogen atom complexes at room temperatures or higher.

Hydrogen, deuterium, and helium are considerably more efficient than predicted. It may be that neon is a rough dividing line between the heavier third bodies which go mainly by the intermediate complex mechanism, and the light third bodies which go mainly by the deactivation mechanism.

Bunker and Davidson (19) have considered a mechanism where all MX complexes, bound or unbound, contribute to the recombination. This calculation can be made by the use of expressions used in virial coefficient theory. For argon and n-butane, they found that this mechanism resulted in greater rates and smaller negative temperature dependences than found by experiments. If applied to helium and hydrogen it gives: $k(He, 50^{\circ}C.) = 7.4 \times 10^{9}$, $k(He, 150^{\circ}C.) = 9.1 \times 10^{9}$, $k(H_2, 50^{\circ}C.) = 7.9 \times 10^{9}$, and $k(H_2, 50^{\circ}C.) = 9.2 \times 10^{9}$. These are larger than the observed rates and actually have a small positive temperature dependence. It may be that for helium and hydrogen, since the bound IM theory gives a small rate, there is a large contribution from the unbound complexes.

3. The More Efficient Third Bodies

Third bodies which are about ten or more times as efficient as argon will be considered in this section. The rates of such third bodies generally lie below the dashed line in figure 8. The more efficient third bodies also lie above the line for "inert gases" in the plot (figure 7) of normal boiling point vs. rate constant. Although the intermediate complex rates are calculated assuming spherical symmetry, this assumption might not be expected to result in errors greater than a factor of two. The reason for these rates to lie below the dashed line is probably due to greater than van der Waals forces between the third body atom and the halogen atom.

In the case of iodine molecules (and possible nitric oxide) as third bodies, it seems quite clear that the intermediate complex is bound by much stronger forces. As the temperature is increased, iodine efficiency falls rapidly and presumably approaches the calculated intermediate complex value. The shock tube data of Britton, et al. (2) indicate that, $k(I_2, 1300^{\circ}K.) \lesssim 1.4 \times 10^{10}$. Intermediate complex theory gives a value of 1.9×10^{10} at this temperature.

The large rate constant for benzene and its moderately large negative temperature dependence suggests that there is some special interaction between an iodine atom and a benzene molecule. It is interesting to note that there is evidence for complexes of molecular iodine in benzene solutions. Russell and Simons (4) have measured

the efficiencies of toluene, p-xylene, and mesitylene at 20°C. and find them to be 2.4, 3.8, and 4.7 times, respectively, as efficient as benzene. More recently, Porter and Smith (23) have found that the temperature dependence of mesistylene efficiency corresponds to $\Delta H = -4.1$ kcal/mole. This compares with $\Delta H = -1.97$ kcal/mole (equation 22) for benzene. The presence of methyl groups on the benzene ring enhances the formation of iodine atom-aromatic ring complexes, as do their presence in the formation of iodine molecule-aromatic ring complexes.

Hydrogen iodide and ethyl iodide are both known to form complexes in solution with molecular iodine (24, 25), and similar complexes with atomic iodine might be expected in recombination experiments with iodides. The recombination rate with hydrogen iodide is somewhat larger than predicted by the intermediate complex theory, and thus a "stable" complex such as HI_2 probably does not play a major role. The recent data of Porter and Smith (23) indicate a probable value of $\Delta H = -2.4$ kcal/mole for ethyl iodide efficiency. Equation 24 gives $\Delta H = -2.55$ kcal/mole for methyl iodide efficiency. The intermediate complex theory considerably underestimates the rates and their negative temperature dependences for methyl and ethyl iodides. These relatively large rates could be accounted for by the formation of iodide-iodine atom complexes stronger than the assumed van der Waals' forces.

4. Other Mechanisms

Another possible factor in iodine atom recombination is the influence of weakly bound states of the iodine molecule. In addition to the $^1\Sigma$ ground state, there is experimental and theoretical evidence (26) for $^3\Pi_2$ and $^3\Pi_1$ bound states in iodine which would also dissociate to $^2P_{3/2}$ iodine atoms. The best estimates for the binding energies of these states are:

(32)

$^1\Sigma$	35.56 kcal/mole
$^3\Pi_2$	0.35 kcal/mole
$^3\Pi_1$	0.14 kcal/mole

The recombining $^2P_{3/2}$ iodine atoms may approach along the potential curve and then be deactivated by collisions. Alternately, they may approach along the $^3\Pi_2$ or $^3\Pi_1$ potential curves. Then they will either be deactivated into the $^1\Sigma$ ground state or dissociate back to free $^2P_{3/2}$ iodine atoms. These arguments are made with the deactivation mechanism in mind (equations 26 and 27), but should generally apply to the intermediate complex mechanism as well.

The rate of dissociation of a molecule may be very roughly represented by:

(33) $$k_D \approx Z \left(\frac{\Delta E}{RT}\right)^{s-1} (s-1)!^{-1} e^{-\Delta E/RT}$$

where ΔE is the binding energy of the bond broken and s is some

measure of the number of internal degrees of freedom. If s = 1, then the ratio of dissociation rates from Π states to the ground state is:

$$\frac{k_D\ (\Pi)}{k_D\ (\Sigma)} = \exp\left[\frac{-E(\Pi) + E(\Sigma)}{RT}\right] \tag{34}$$

This shows that the Π states will dissociate much faster than the ground state; possibly on every few collisions. The rate of deactivation of Π to Σ cannot be calculated, although it probably needs many more collisions than for the dissociation of the Π states. This deactivation requires a transition in total spin which is forbidden in light atoms, but Rabinowitch (25) considers spin-orbit interactions large enough in iodine to make such transitions allowed. The probability that a pair of iodine atoms approach along the Π curves is four times greater than for approach along the $^1\Sigma$ curve, and this may help the Π states to contribute. Such a contribution to the overall rate, if it exists, could also contribute to the observed negative temperature dependence of the third order rate constant.

This introduces another point which has been discussed by Wigner (16), Rabinowitch (17), and others. Since the two $^2P_{3/2}$ iodine atoms have a combined degeneracy of 16, and only one of these may lead directly to the $^1\Sigma$ ground state, it would appear that an "electronic degeneracy" steric factor of 1/16 should be introduced into the rate constant expression. If the Π states can deactivate to the $^1\Sigma$ state with reasonable probability, this steric factor might

be raised to about 5/16. The factor of 1/16 would destroy the agreement of intermediate complex theory with the magnitude of the rate constant. A steric factor of 5/16 could be tolerated since agreement with the inert gas rate constants is improved if the overall steric factor is about 1/4.

5. Nitric Oxide

As described in part IV, only limited experiments were made with nitric oxide, but the recombination rate does appear to be very fast. Three possible explanations are given here.

If nitric oxide is a very efficient third body, it would probably have to be considered similar in mechanism to the iodine molecule third body. Such a mechanism is:

(35) $$I + NO \underset{}{\overset{K}{\rightleftharpoons}} INO$$

(36) $$INO + I \xrightarrow{PZ} I_2 + NO$$

where the intermediate complex, nitrosyl iodide, is not stable under normal conditions, although the corresponding bromide is a partially decomposed liquid at room temperature. If the second reaction is governed by a collision number and a steric factor, P, the overall rate is:

(37) $$k = PZK = \frac{1}{2} ZK$$

where K is the equilibrium constant of the first reaction. The lower limit of k(NO, 50°C.) $\gtrsim 1.8 \times 10^{13}$ found in part IV indicates that the equilibrium constant of the first reaction should be 370 liters/mole (or 14 atm.$^{-1}$) or larger.

Another possibility is that a small concentration of nitrosyl iodide exists in the system before flash photolysis. The iodine atoms produced could then be very rapidly converted back to iodine molecules by the second reaction.

A less probable explanation is the production of some "colored" species (such as INO) which could keep the overall optical density of the system constant. Nitrosyl iodide would suffice for this explanation if its extinction coefficient is about one-half of that for molecular iodine.

Experiments were also made with carbon monoxide, but it exhibited the efficiency expected from an inert gas type interaction. The calculated "inert gas" efficiency of nitric oxide is about the same as the calculated efficiency for carbon monoxide. In conclusion, it seems that the intermediate "strongly bound" complex mechanism is the most plausible explanation for the behavior of nitric oxide. Further experiments with shorter duration flash lamps and possible spectroscopic attempts to identify nitrosyl iodide are suggested by this study.

VI. CLASSICAL ATOM RECOMBINATION COLLISIONS

1. Introduction

A possible approach to the theoretical prediction of atom recombination rates is the detailed calculation of collisions between the recombining atoms and a third body atom. Using classical mechanics and simple intermolecular potentials, the problem is not difficult to formulate, but is difficult to solve in detail, since the differential equations of motion are nonlinear. Only with the aid of the high speed computers has this approach become feasible.

Wall, Hiller, and Mazur (27) have treated the exchange reaction,

(38) $$H + H_2 \longrightarrow H_2 + H$$

The main difficulty is that the potential surface for this reaction is not known in any great detail. By using a "quantum mechanical" potential and classical mechanics, they have determined the outcome of many linear collisions with various initial conditions. This problem has recently been set up in three dimensions by Wall and coworkers (28), using a Monte Carlo technique to select initial conditions. Out of many hundreds of collisions, they find that about 5% lead to exchange.

These interesting calculations of Wall and co-workers have prompted this attempt to treat collisions in three body atom recombinations. The potential surface for atom recombination is probably simpler than for hydrogen exchange. Quantum mechanical effects should generally be small in atom recombinations involving heavy atoms or molecules. The potential for a pair of atoms should be approximately independent of the position of the remaining "inert" third body atom. The primary difficulty at present is not the numerical solution of the equations of motion, but is in the number of initial conditions. There are 8 initial conditions to vary in the three dimensional collisions, 5 in the two dimensional, and 3 in the linear collisions. For this reason, present calculations have been limited to linear collisions. Such linear collisions neglect any importance of the angular momentum, which may be quite important in actual collision processes. The linear collisions studied here were:

$$I + I + A \quad \text{and} \quad IA + I$$

where IA is in the non-vibrating bound state.

2. Theory

Consider three particles in the coordinate system in figure 9.

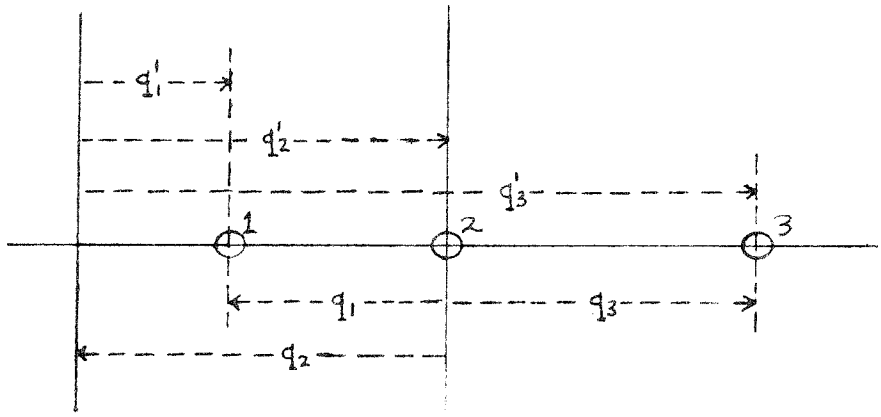

Figure 9

The classical Hamiltonian for these particles in the primed system is:

$$(39) \qquad H' = \sum_{i=1}^{3}\left[\frac{1}{2}m_i q_i'^2 + V(q_i')\right] = \sum_{i=1}^{3}\left[\frac{p_i'^2}{2m_i} + V(q_i')\right]$$

where $V(q_i')$ is the potential function between these particles. It is desirable to transfer to the unprimed coordinate system with the origin at the middle particle. This can be done by the following set of transformations:

$$(40) \qquad \begin{aligned} q_1' &= q_1 - q_2 & p_1' &= p_1 \\ q_2' &= -q_2 & p_2' &= p_2 + p_1 + p_3 \\ q_3' &= q_3 - q_2 & p_3' &= p_3 \end{aligned}$$

Then the transformed Hamiltonian and canonical equation are:

$$(41) \qquad H = \frac{1}{2}\left[\frac{p_1^2}{m_1} + \frac{(p_2 + p_1 + p_3)^2}{m_2} + \frac{p_3^2}{m_3}\right] + V(q_1)$$

$$(42) \qquad \frac{dq_r}{dt} = \frac{\partial H}{\partial p_r} \qquad \frac{dp_r}{dt} = -\frac{\partial H}{\partial q_r} \qquad (r = 1, 2, 3)$$

Since $H \neq H(q_2)$, the corresponding momentum, p_2, may be equated to zero without loss of generality. Then the equations of motion become:

$$(43) \qquad v_1 = \frac{dq_1}{dt} = \left[\frac{1}{m_1} + \frac{1}{m_2}\right] p_1 + \left[\frac{1}{m_2}\right] p_3$$

$$(44) \qquad v_3 = \frac{dq_3}{dt} = \left[\frac{1}{m_2}\right] p_1 + \left[\frac{1}{m_2} + \frac{1}{m_3}\right] p_3$$

$$(45) \qquad \frac{dp_1}{dt} = -\frac{\partial V(q_1)}{\partial q_1} \qquad \frac{dp_3}{dt} = -\frac{\partial V(q_3)}{\partial q_3}$$

This set of four nonlinear simultaneous differential equations can be reduced to only two equations by eliminating the time dependence, but this was not advantageous in these calculations.

It will be necessary to specify four initial conditions to start the solution of this set of equations. At $t = 0$, the relative positions of particles 1 and 3 may be specified, and it is convenient to specify their relative initial velocities. The explicit expression for the momentum in terms of the velocities were obtained by inverting equations 43 and 44.

(46) $$p_1 = \frac{m_1\left[(m_2 + m_3)\, v_1 - m_3 v_3\right]}{m_1 + m_2 + m_3}$$

(47) $$p_2 = \frac{m_3\left[-m_1 v_1 + (m_1 + m_2)\, v_3\right]}{m_1 + m_2 + m_3}$$

These relations are useful in the numerical calculations described in the next section.

For the purposes of these calculations, the particle 1 will always be the third body atom, and particles 2 and 3 will be the iodine atoms. The potential between the third body atom and the iodine atoms was taken to be a Lennard-Jones potential:

(48) $$V_{12}(q_1) = 4\epsilon\left[\left(\frac{\sigma}{q_1}\right)^{12} - \left(\frac{\sigma}{q_1}\right)^{6}\right]$$

The potential, $V_{13}(q_1 - q_3)$, will always be slightly attractive for linear collisions and not very important, but it was included in these calculations. For nonlinear collisions, it would always be necessary to include V_{13}. The values for ϵ and σ were obtained by using the combining rules as described in part V. For iodine and argon, the values used were $\epsilon = 162.5°K.$ and $\sigma = 3.753\ \text{Å}$.

The iodine-iodine interaction was described by a Morse potential with constants derived from the data of Herzberg (29).

(49) $$V_{23}(q_3) = D\left[e^{-2a(q_3 - r_e)} - 2\, e^{-a(q_3 - r_e)}\right]$$

The parameters used were, $D = 2.4698 \times 10^{-12}$ ergs, $a = 1.866\ \text{Å}^{-1}$,

and $r_e = 2.667$ Å. It is interesting to note that the maximum depth of this Lennard Jones potential is only 1/100 the maximum depth of this Morse potential.

There are four initial conditions for this linear collision problem, but one condition need not be varied. Both q_1 and q_3 may be initially taken large enough so that the potentials between the corresponding atoms are initially negligible. Then the one initial distance and both initial velocities can be varied to obtain a distribution of possible collisions. The initial velocities should correspond to a range of thermal velocities and the interatomic distances taken over a range large enough to include all interesting features of the collisions for given initial velocities.

The information obtained from this type of calculation might be generally represented as a function, $P(q_1 \cdots q_{3n}, p_1 \cdots p_{3n})$. The value of this function would be unity for collisions resulting in recombination, and zero for collisions resulting in dissociation. It would then be necessary to integrate $P(q's;p's)$ with a statistical weighting function to obtain the "steric" factor for the three body collisions. In very general notation, this steric factor would be,

$$(50) \quad \frac{1}{N}\int\cdots\int P(q_1 \cdots q_{3n}, p_1 \cdots p_{3n}) \; e^{-H(q_1 \cdots q_{3n}, p_1 \cdots p_{3n})/kT} \; dq_1 \cdots dq_{3n} dp_1 \cdots dp_{3n}$$

where N is a normalising factor. To obtain the rate it would be

necessary to multiply this steric factor by a three body collision number. A more generally correct rate would be obtained by considering the rate at which systems cross a surface in phase space. If this surface is considered at $q_1 = q_1^0$, the rate would be

$$k \propto \int \cdots \int P(q_1^0, q_2 \cdots q_{3n}, p_1 \cdots p_{3n})\, e^{-H(q_1^0, q_2, \cdots q_{3n}, p_1 \cdots p_{3n})/kT} \dot{q}_1\, dq_2 \cdots dq_{3n}\, dp_1 \cdots dp_{3n} \tag{51}$$

It is also of interest to examine the energy distribution after the collision, i.e., the amount of energy in the recombined molecule if recombination has taken place.

3. Computation

All calculations of these collisions were done on an Electro-Data 205 digital computer, using a modified numerical integration scheme programmed by Taylor (30). The fourth order Runge-Kutta integration (31) as modified by Gill (32) was programmed to solve as many as 19 simultaneous first order nonlinear differential equations. The interval of integration was not fixed but could be changed during a calculation, either manually or by an internal error check routine. This error check routine would either halve or double the integration interval, depending on if the error in integration was greater or less than a given error tolerance. The computation would stop when an interatomic distance increased past a certain preset distance, and

then continue with a new set of initial conditions. The initial relative velocities, v_1^o and v_3^o, were introduced into the input data of the computer and the corresponding momentum, p_1^o and p_3^o, were calculated by a routine using equations 46 and 47. If recombination takes place, the energy remaining in the iodine molecule may be calculated from the maximum extension of the vibrating molecule.

Although all calculations were done in "floating point" arithmetic and "scaling" was not essential, it was convenient to define a new set of units. All lengths were specified in Angstroms, all masses in atomic mass units, and all times in units of $\mu\mu$ seconds (10^{-12} sec.). Then the c.g.s. energy may be converted into the new units (1 erg = 6.0228×10^{15} new energy units).

For the collisions considered here, it was found that a satisfactory initial interval of integration was 1×10^{-2} $\mu\mu$ sec. This initial interval was then adjusted by the program in accordance with the error check routine. A complete collision took from 10 to 30 minutes of computer time, depending on the initial conditions. The calculation for a single interval took about 5 seconds.

4. Discussion

The collision between the IA complex and an I atom are of interest since the intermediate complex theory assumes a steric factor of 1/2 for the second step (equation 29). If this steric factor is considerably less than 1/2, the magnitude of the calculated rates

would be too small to agree with experimental rates. As a preliminary investigation, the I + IA linear collision was tried. If the IA complex is taken to have no initial internal energy, the relative velocity of approach is the only initial condition to vary. The calculation was run for various velocities ranging between 0.5 to 8.0×10^4 cm./sec., which are in the range of thermal gas velocities.

The results of the I + IA linear collisions are shown in table 5. Some typical collision trajectories are plotted in figure 10 for various velocities. The motion appears as it would to an observer located on the central iodine atom. Although this is not a complete picture of even the linear collisions, it appears that the steric factor may well be of the order of 1/2. The outcome of three dimensional collisions with angular momentum and vibrating IA cannot be predicted from these results.

Some calculations were also made on I + I + A linear collisions, where now three initial conditions can be varied independently. Collisions were made with fixed initial velocities, and the interatomic distance was varied. The iodine-iodine distance was kept fixed at $q_3^o = 10$ Å., and the iodine-argon distance was varied between 6 and 22 Å. The initial velocities were, $v_1^o = 9.06 \times 10^4$ cm./sec. and $v_3^o = -8.14 \times 10^4$ cm./sec. Table 6 gives the results of these collisions and some typical trajectories are shown in figure 11. No general conclusions can be drawn from this set of collisions,

Table 5

I + IA Linear Collisions

Velocity	Results	Energy in I_2*
0.5×10^4 cm./sec.	Recombination	0.69
1.0	Dissociation	---
1.5	Recombination	0.93
2.0	Recombination	0.68
3.0	Recombination	0.71
4.0	Recombination	0.97
5.0	Recombination	0.78
6.0	Dissociation	---
7.0	Recombination	0.82
8.0	Recombination	0.73

*Fraction of the dissociation energy remaining in the I_2 after collision.

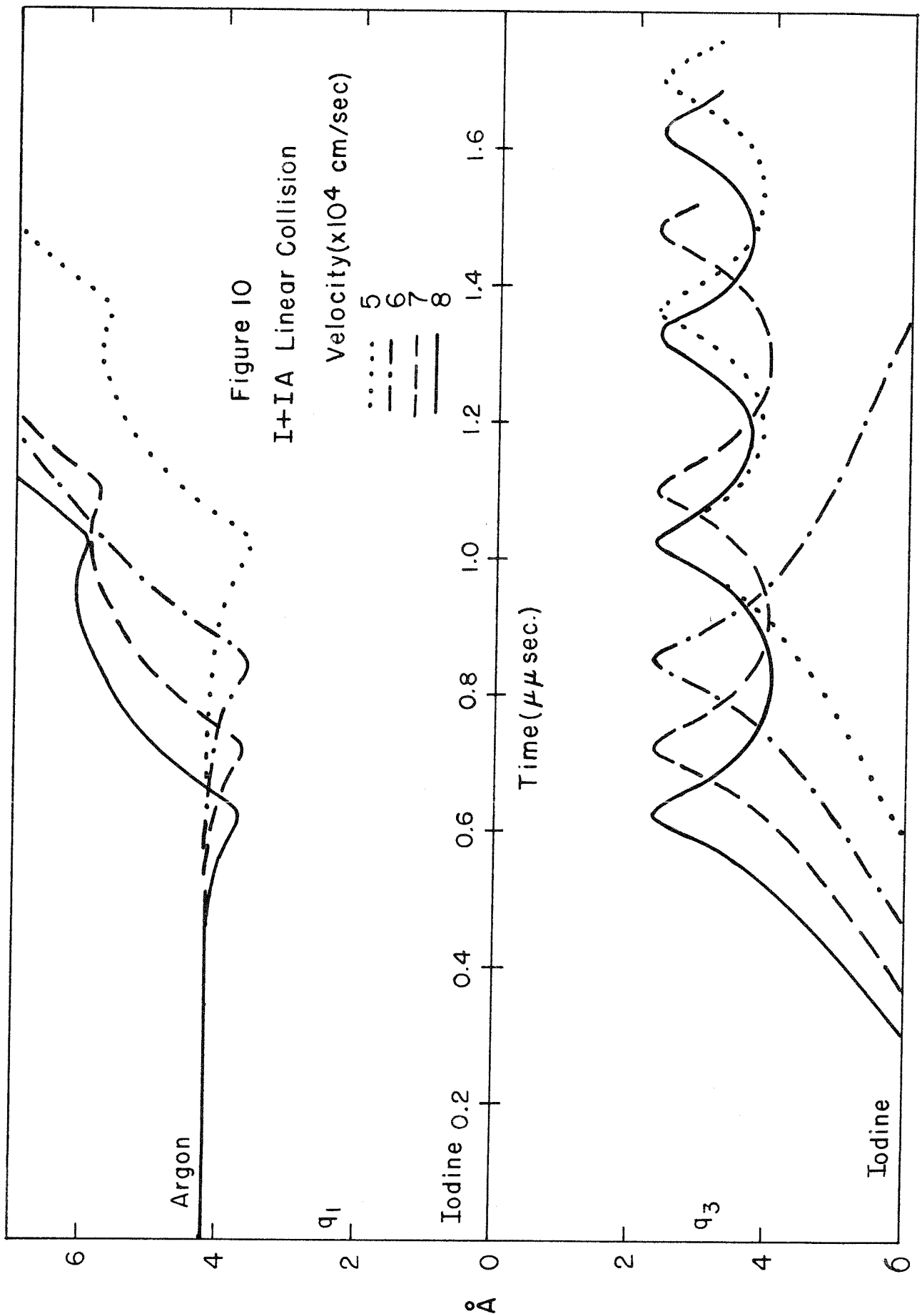
Figure 10
I+IA Linear Collision
Velocity(x10⁴ cm/sec)
5
6
7
8
Argon
Iodine
Iodine
q_1
q_3
Time($\mu\mu$sec.)
0.2
0.4
0.6
0.8
1.0
1.2
1.4
1.6
Å
0
2
4
6
2
4
6

Table 6

I + I + A Linear Collisions

$v_1^o = 9.06 \times 10^4$ cm./sec. $v_3^o = -8.14 \times 10^4$ cm./sec. $q_3^o = 10$ Å.

q_1^o	Results	Energy in I_2*
-6.0 Å.	Recombination	0.84
-6.5	Dissociation	---
-7.0	"	---
-7.5	"	---
-8.0	"	---
-8.5	"	---
-9.0	"	---
-9.5	Recombination	0.76
-10.0	"	0.68
-11.0	"	0.48
-12.0	"	0.57
-13.0	"	0.69
-14.0	"	0.98
-16.0	"	0.99
-18.0	"	0.99
-20.0	Dissociation	---
-22.0	"	---

$v_1^o = 4.10 \times 10^4$ cm./sec. $v_3^o = -2.30 \times 10^4$ cm./sec. $q_3^o = 10$ Å.

q_1^o	Results	Energy in IA**
-8.0 Å.	IA formed (?)	---
-10.0	IA formed	0.78

*Fraction of the dissociation energy remaining in the I_2 after collision.
**Fraction of the binding energy remaining in IA after collision.

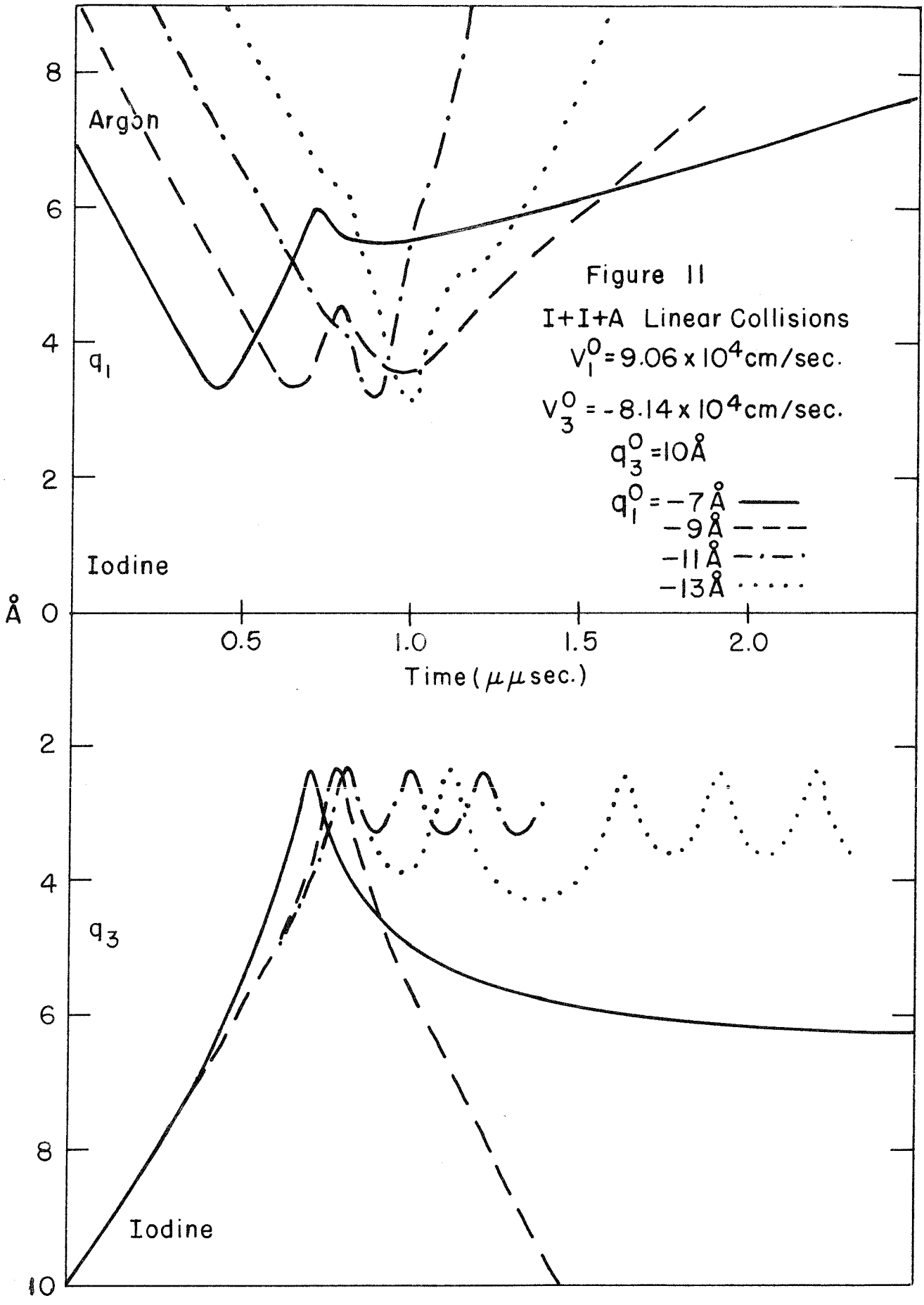

Figure 11

I+I+A Linear Collisions

$V_1^0 = 9.06 \times 10^4$ cm/sec.

$V_3^0 = -8.14 \times 10^4$ cm/sec.

$q_3^0 = 10$ Å

$q_1^0 = -7$ Å ——

-9 Å – – –

-11 Å –·–·

-13 Å ·····

although it is interesting to note that recombination processes do not occur only in one definite range of q_1^o. From q_1^o = -9.5 Å. to -10.0 Å. there is a decrease in the energy remaining in the iodine molecule, followed by an increase until -18.0 Å., where dissociation takes over.

Two collisions with lower velocities of $v_1^o = 4.10 \times 10^4$ cm./sec. and $v_3^o = -2.30 \times 10^4$ cm./sec. were run. At least one of these shows the definite formation of the IA complex with its relatively long period of vibration.

The calculations presented here are only a preliminary attempt to outline a general problem which can probably be successfully attacked in the next few years. The new computers (possibly 10^4 times "faster" than used here) will allow the computation of many thousands of two or three dimensional collisions which can be averaged over the proper distributions.

APPENDIX

1. Rate of Hydrogen Iodide Formation and Decomposition.

The experimentally derived equation(33) for the rate constant of the reaction:

(52) $$H_2 + I_2 \xrightarrow{k} 2\,HI$$

is:

(53) $$\log\left(\frac{k}{T^{1/2}}\right) = 9.73 - \frac{40740}{4.575\,T} \qquad k \text{ in } \frac{\text{liters}}{\text{mole sec.}}$$

Then the initial rate of formation of hydrogen iodide from a mixture of hydrogen and iodine vapor is:

(54) $$-\frac{d[HI]}{dt} = 2k[H_2][I_2] \qquad [HI] = 2tk[H_2][I_2]$$

For typical conditions (P_{H_2} = 500 mm., P_{I_2} = 0.3 mm.), the concentration of hydrogen iodide formed in one hour is given in table 7 .

If K is the equilibrium constant of the first reaction, the initial rate of hydrogen iodide decomposition is:

(55) $$-\frac{d[HI]}{dt} = 2kK[HI]^2 \qquad \Delta[HI] = 2tkK[HI]^2$$

For a typical hydrogen iodide pressure of 200 mm., the rate of decomposition and the quantity decomposed in one hour is given in

table 8.

Table 7

Rate of Hydrogen Iodide Formation

Temperature	$[H_2]$(m/l)	$[I_2]$(m/l)	k (l/m sec.)	[HI] per hour
50°C.	2.48×10^{-2}	1.49×10^{-5}	3.06×10^{-14}	8.0×10^{-20} m/l
150	1.90×10^{-2}	1.14×10^{-5}	1.16×10^{-10}	1.6×10^{-13} m/l
275	1.46×10^{-2}	8.78×10^{-6}	7.93×10^{-6}	7.8×10^{-9} m/l

Table 8

Rate of Hydrogen Iodide Decomposition

Temperature	[HI] (m/l)	kK (l/m sec.)	Δ[HI] per hour
50°C.	9.93×10^{-3}	1.98×10^{-11}	1.4×10^{-11} m/l
150	7.58×10^{-3}	2.82×10^{-8}	1.2×10^{-8} m/l
275	5.86×10^{-3}	8.73×10^{-4}	2.2×10^{-4} m/l

2. Energy Levels of a Double Molecule

A double molecule is a pair of atoms (or molecules) which are held together by weak van der Waals forces. The object is to develop a method for the location of the bound vibrational energy levels in the potential well. Since intramolecular potentials are approximated by a harmonic oscillator potential, for which the W.K.B. method gives exact solutions, the W.K.B. method was used to obtain a set of approximate solutions.

Since the potentials are to be spherically symmetric, it is only necessary to consider the radial wave equation:

$$(56)\quad -\frac{\hbar^2}{2}\left[\frac{1}{r^2}\frac{d}{dr}\left(r^2\frac{d}{dr}\right) - \frac{l(l+1)}{r^2}\right]\psi(r) - \left[E - U(r)\right]\psi(r) = 0$$

After the usual transformation, $\psi(r) = r^{-1}R(r)$, and using reduced distances, $u = r/\sigma$, this equation becomes:

$$(57)\quad -K^2\left[\frac{d^2}{du^2} - \frac{l(l+1)}{u^2}\right]R(u) - \left[\epsilon - V(u)\right]R(u) = 0 \qquad K = \frac{\hbar}{\sigma\sqrt{2\mu\epsilon_0}}$$

where $V(u)$ is a reduced potential of maximum depth -1, σ is a characteristic distance of the potential, μ is the reduced mass of the double molecule, ϵ_0 is the maximum depth of the "unreduced" potential, and $\epsilon = E/\epsilon_0$ so that ϵ varies from zero (at the top of the well) to -1 (at the bottom of the well) for bound states. If the angular momentum quantum number is zero, the W.K.B. solution is (34):

(56) $$K\pi(v+\tfrac{1}{2}) = \oint \sqrt{\epsilon - V(u)}\, du$$

where v is the vibrational quantum number and the integral is evaluated between the classical turning points, i.e., the roots of $\epsilon - V(u) = 0$.

Since these calculations may be useful for purposes other than described in this thesis, the numerical calculations have been extended to several often used intermolecular potentials. The two reduced potential forms to be considered are the Lennard Jones:

(59) $$V(u) = M\left[u^{-m} - u^{-n}\right] \qquad M = \left[\frac{n}{m-n}\right]\left[\frac{m}{n}\right]^{\left(\frac{m}{m-n}\right)}$$

and the modified Buckingham (6-exp):

(60) $$V(u) = \frac{1}{1 - 6/\alpha}\left[\frac{6}{\alpha}\, e^{\alpha(1-u)} - u^{-6}\right] .$$

For the Lennard Jones, σ is the distance between the origin and the zero of the potential, while for the Buckingham, σ is the distance between the origin and the minimum of the potential. These potentials can be used in equation 58, and the resulting integral will be called the W.K.B. integral, I_ϵ .

In general, these W.K.B. integrals defy analytical solution, but the Lennard Jones form can be integrated exactly for the special case when $\epsilon = 0$. Then the integral becomes:

$$(61) \qquad K\pi\left(v + \frac{1}{2}\right) = M^{1/2} \int_1^\infty \sqrt{-u^{-m} + u^{-n}}\, du$$

Stogryn and Hirschfelder (22) have also considered this integral (with m = 12 and n = 6) to obtain the maximum number of energy levels in a given potential well, but their method of integration is somewhat more complicated. If the substitution, $x = u^{(n-m)}$, is made, the resulting integral is a simple Beta function (35):

$$(62) \quad K\pi\left(v + \frac{1}{2}\right) = \frac{M^{1/2}}{(m-n)} B\left[\frac{\frac{n}{2}}{n-m} ; \frac{3}{2}\right] \quad \text{when} \quad \epsilon = 0$$

Since the Beta function can be written in terms of Gamma functions, this expression can easily be evaluated. For the other integrals, Weddle's numerical integration (36) was programmed on an Electro-Data 205 digital computer and the integrals evaluated in 0.02 intervals in ϵ. Convergence to at least four significant figures was obtained by decreasing the interval of integration. Tables 9 and 10 show the results of all integrations for the various reduced potentials. Four of these integrals are plotted as functions of the reduced energy in figure 12. These are the first general numerical solutions for these potentials, and it is interesting to compare these with some special solutions.

Kihara (37) has found an exact solution of equation 57 for the

Table 9

W.K.B. Integral as a Function of Energy for the Lennard Jones Potential

ϵ	m = 9 n = 6	m = 10 n = 6	m = 12 n = 6
0	0.9602	0.9108	0.8413
-0.02	.7137	.6748	.5691
-0.04	.6486	.6128	.5176
-0.06	.6023	.5689	.4812
-0.08	.5652	.5337	.4512
-0.10	.5336	.5037	.4272
"	.5056	.4774	.4054
"	.4809	.4538	.3859
"	.4581	.4323	.3680
"	.4372	.4124	.3515
-0.20	.4176	.3939	.3361
"	.3992	.3765	.3216
"	.3818	.3601	.3079
"	.3654	.3445	.2949
"	.3497	.3297	.2825
-0.30	.3347	.3155	.2707
"	.3203	.3020	.2593
"	.3065	.2889	.2483
"	.2932	.2763	.2377
"	.2803	.2642	.2275
-0.40	.2679	.2525	.2176
"	.2558	.2411	.2080
"	.2441	.2300	.1986
"	.2327	.2193	.1895
"	.2216	.2089	.1806
-0.50	.2109	.1987	.1720
"	.2003	.1888	.1635
"	.1901	.1791	.1552
"	.1800	.1696	.1472
"	.1702	.1604	.1392
-0.60	.1606	.1513	.1315
"	.1512	.1425	.1239
"	.1420	.1338	.1164
"	.1329	.1252	.1091
"	.1241	.1169	.1018
-0.70	.1154	.1087	.09476
"	.1068	.1006	.08779
"	.09840	.09269	.08093
"	.09013	.08489	.07417
"	.08120	.07723	.06752
-0.80	.07400	.06969	.06096
"	.06611	.06226	.05450
"	.05834	.05495	.04813
"	.05069	.04774	.04184
"	.04315	.04064	.03564
-0.90	.03572	.03364	.02952
"	.02838	.02673	.02347
"	.02115	.01992	.01750
"	.01401	.01319	.01160
"	.006960	.006554	.005765
-1.00	.0000	.0000	.0000

Table 10

W.K.B. Integral as a Function of Energy for the Buckingham Potential

ϵ	$\alpha = 12$	$\alpha = 13$	$\alpha = 14$	$\alpha = 15$
0	0.8178	0.7969	0.7791	0.7642
-0.02	.5691	.5488	.5322	.5185
-0.04	.5176	.4982	.4823	.4692
-0.06	.4812	.4625	.4473	.4346
-0.08	.4520	.4340	.4193	.4070
-0.10	.4272	.4098	.3956	.3837
	.4054	.3886	.3749	.3633
	.3859	.3696	.3563	.3451
	.3680	.3523	.3394	.3285
	.3515	.3363	.3238	.3133
-0.20	.3361	.3214	.3093	.2991
	.3216	.3073	.2957	.2858
	.3079	.2941	.2828	.2733
	.2949	.2816	.2707	.2614
	.2825	.2697	.2591	.2501
-0.30	.2707	.2583	.2480	.2394
	.2593	.2473	.2374	.2291
	.2483	.2367	.2272	.2191
	.2377	.2266	.2174	.2096
	.2275	.2168	.2079	.2004
-0.40	.2176	.2073	.1987	.1915
	.2080	.1980	.1898	.1829
	.1986	.1891	.1812	.1745
	.1895	.1803	.1728	.1664
	.1806	.1719	.1646	.1585
-0.50	.1720	.1636	.1567	.1508
	.1635	.1555	.1489	.1433
	.1552	.1476	.1413	.1359
	.1472	.1399	.1339	.1288
	.1392	.1323	.1266	.1218
-0.60	.1315	.1249	.1195	.1149
	.1239	.1177	.1125	.1082
	.1164	.1106	.1057	.1016
	.1091	.1036	.09902	.09514
	.1018	.09671	.092444	.08881
-0.70	.09476	.08996	.08598	.08259
	.08779	.08333	.07963	.07647
	.08092	.07680	.07338	.07047
	.07417	.07039	.06724	.06455
	.06752	.06406	.06119	.05873
-0.80	.06096	.05783	.05523	.05301
	.05450	.05169	.04936	.04737
	.04813	.04564	.04358	.04181
	.04184	.03968	.03788	.03634
	.03564	.03379	.03225	.03094
-0.90	.02952	.02798	.02670	.02561
	.02347	.02224	.02123	.02036
	.01750	.01658	.01582	.01517
	.01160	.01099	.01048	.01005
	.005765	.005462	.005209	.004994
-1.00	.0000	.0000	.0000	.0000

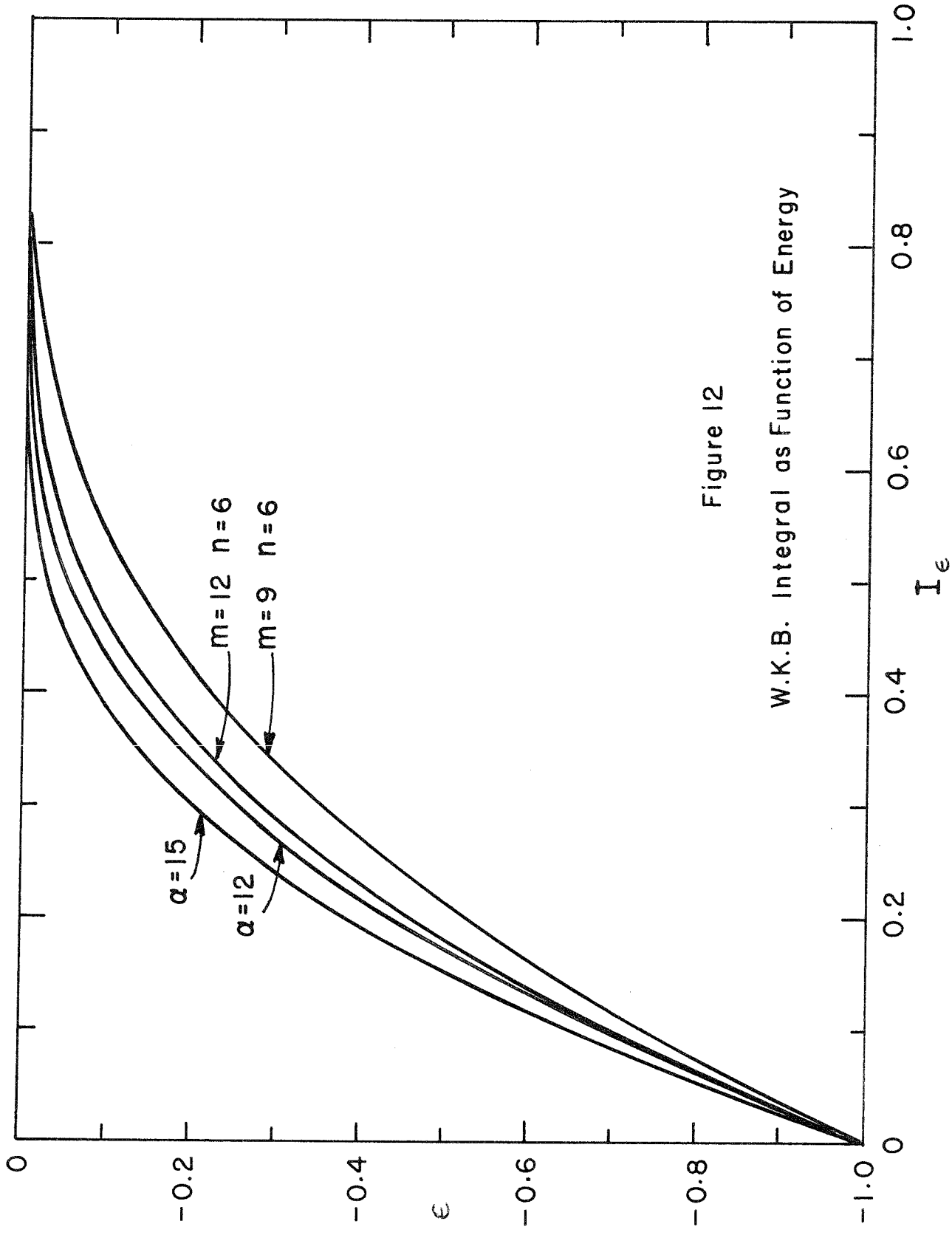

Figure 12

W.K.B. Integral as Function of Energy

Lennard Jones potential form, provided that $\epsilon = \nu = \ell = 0$. If a trial function of the form, $R(u) = e^{-b/r^a}$, is chosen, and substituted into equation 57 (with $\epsilon = \ell = 0$), it is then possible to adjust the parameters a and b so that this R(u) is a true solution. In order to do this, the following conditions emerge:

(63) $m = 2n - 2 \quad a = (m - 2)/2 \quad b = m/(m - 2) \quad K = 2\, M^{\frac{1}{2}}/m$

Thus there are exact zero energy solutions for two cases of possible interest, namely, $m = 10$, $n = 6$ and $m = 12$, $n = 7$.

Kilpatrick and Kilpatrick(38) have obtained variation method solutions of the Lennard Jones ($m = 12$, $n = 6$) potential when $\nu = \ell = 0$. The values of K from these sources and the W.K.B. method are compared in table 11 when $\epsilon = \ell = \nu = 0$. While the error is large in these limiting cases, the error will decrease rapidly as ϵ decreases and ν increases.

Table 11

Lennard Jones Potential	Exact Solution	W.K.B. Solution	% Error in K
$m = 12$ $n = 6$	$K = 0.423$	$K = 0.536$	-26.7
$m = 12$ $n = 7$	$= 0.376$	$= 0.452$	-20.2
$m = 10$ $n = 6$	$= 0.463$	$= 0.580$	-25.3

For the Lennard Jones ($m = 12$, $n = 6$) potential, a detailed plot (figure 13) is shown of the energy level structure as a function of

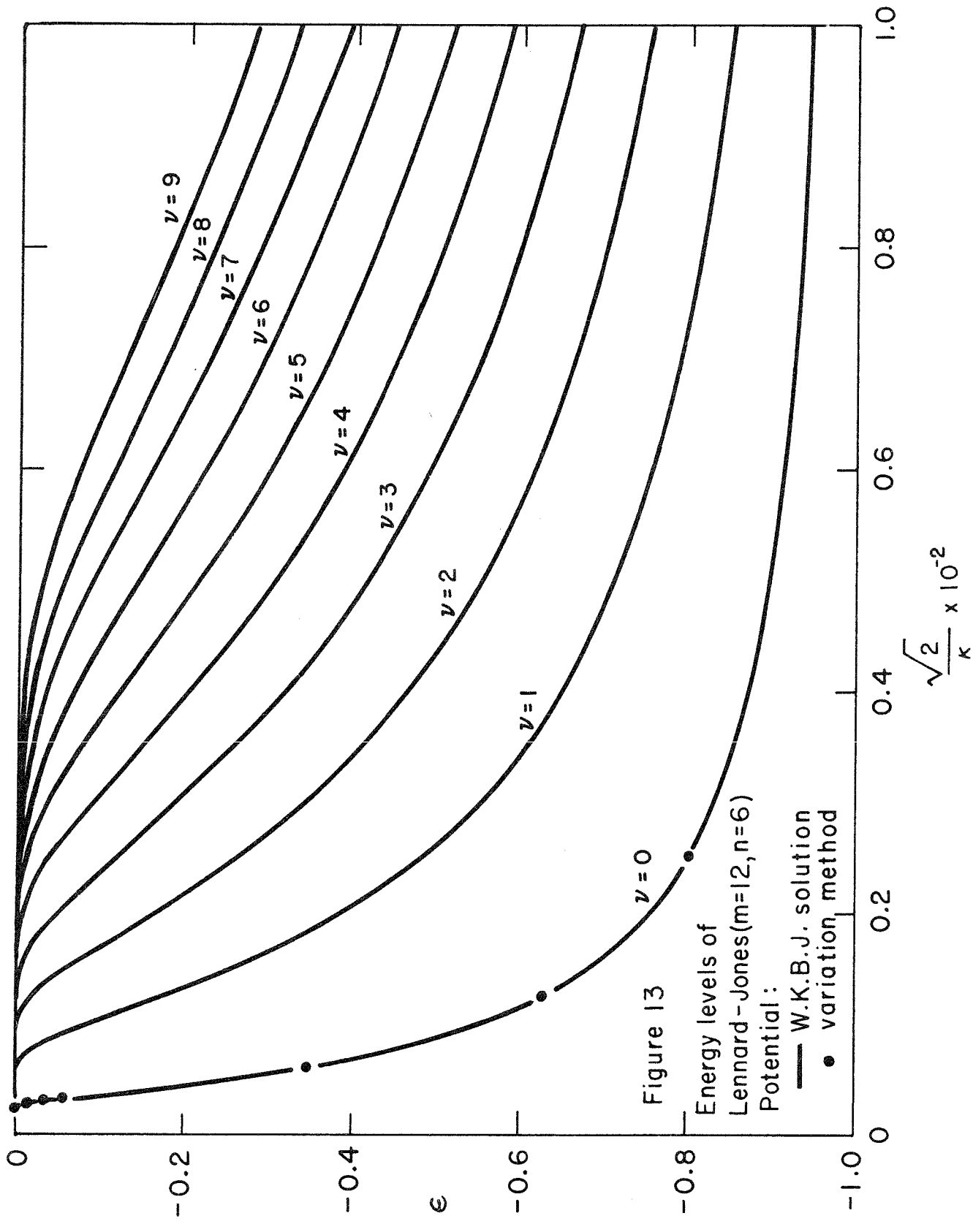
0
-0.2
-0.4
-0.6
-0.8
-1.0
ε
0
0.2
0.4
0.6
0.8
1.0
$\frac{\sqrt{2}}{\kappa}$ x 10^{-2}
ν = 0
ν = 1
ν = 2
ν = 3
ν = 4
ν = 5
ν = 6
ν = 7
ν = 8
ν = 9
Energy levels of
Lennard-Jones(m=12, n=6)
Potential :
— W.K.B.J. solution
• variation method

Figure 13

$1/K$. A few variation method solutions of Kilpatrick and Kilpatrick (38) are also shown. These W.K.B. solutions provide a convenient method for the rapid calculation of the energy levels of a double molecule, except for some error near $\epsilon = 0$.

3. Equilibrium Constants for Double Molecules

Bunker and Davidson (19), Stogryn and Hirschfelder (22), and Britton (39) have calculated equilibrium constants for loosely bound double molecules. The first two papers deal with classical statistical mechanics and the Lennard Jones potential, while the last paper uses quantum statistics and a Morse potential. Quantum statistics have been used here to calculate equilibrium constants of double molecules bound by a Lennard Jones potential.

The equilibrium considered is:

$$(64) \qquad M + X \underset{\longleftarrow}{\overset{K}{\longrightarrow}} MX \qquad K = \frac{[MX]}{[M]\ [X]} = \frac{Q_{MX}}{Q_M\ Q_X}$$

where the Q's are the partition functions of the various species. The usual translational partition functions may be substituted, leaving only the internal partition function for MX to be evaluated.

$$(65) \qquad K = \left(\frac{h^2}{2\pi\mu\ kT} \right)^{3/2} Q_{MX}\ (\text{internal})$$

The rotational partition function for an oscillator is,

$$(66) \qquad Q_{MX}\ (\text{rot.}) = \sum_{l=0}^{l_{max.}} (2l + 1)\, e^{-l(l+1)\,\epsilon_r/kT}$$

where ℓ is the angular momentum quantum number and ϵ_r is the rotational energy level spacing. For a rigid rotor,

(67) $$\epsilon_r = \frac{\hbar^2}{2\mu r_0^2} = \frac{\hbar^2}{2^{4/3}\mu\sigma^2}$$

where r_0 is at the minimum of the potential well. This summation over the rotational states may be replaced by an integration if $\epsilon_r \ll kT$. Such an integration should be made between the limits of $\ell = 0$ and $\ell_{max.}$. $\ell_{max.}$ should be such that the total internal energy is not greater than the binding energy of MX. This requirement gives the relationship,

(68) $$\epsilon_v + \epsilon_r \ell_{max.}(\ell_{max.} + 1) = 0$$

where ϵ_v is the location of the v th vibrational energy level. The substitution of $x = \ell(\ell + 1)\epsilon_r/kT$ makes possible the integration of equation 66 and yields:

(69) $$Q_{MX(rot.)} = \frac{kT}{\epsilon_r}\left[1 - e^{\epsilon_v/kT}\right]$$

The vibrational partition function will be taken as a sum over the energy levels with the rotational partition function included in the sum. This sum is terminated with $v_{max.}$, the uppermost energy level

(70) $$K = \left(\frac{\hbar^2}{2\pi\mu kT}\right)^{3/2} \sum_{v=0}^{v_{max.}} e^{-\epsilon_v/kT} \frac{kT}{\epsilon_r}\left[1 - e^{\epsilon_v/kT}\right]$$

of the bound double molecule. This is equivalent to the assumption of Bunker and Davidson (19) that the total internal energy be no greater than the binding energy of M_2. Equation 70 may be reduced to:

$$K = \frac{2^{7/3}\pi\hbar\sigma^2}{(2\pi\mu kT)^{1/2}} \sum_{v=0}^{v_{max.}} \left[e^{-\epsilon_v/kT} - 1 \right] \tag{71}$$

If $-\epsilon_v \ll kT$, equation 71 reduces to,

$$K = \frac{2^{11/6}\pi^{1/2}\hbar\sigma^2}{\mu^{\frac{1}{2}}(kT)^{3/2}} \sum_{v=0}^{v_{max.}} (-\epsilon_v) \tag{72}$$

When this last K is combined with the $T^{-\frac{1}{2}}$ dependence of the collision number, the same $1/T$ dependence of the third order rate is obtained as from equation 30 when $\epsilon_o \ll kT$. If $-\epsilon_v \gtrsim kT$, the temperature dependence will approximately follow an Arrhenius type equation.

Equation 71 was used to evaluate K for several double molecules using ϵ_v from appendix 2. The expression for K (equation 57) and equation 71 were reduced to numerical conversion factors in convenient units.

$$K = 4.915/\sigma(\mu\epsilon_o)^{1/2} \tag{73}$$

$$K = 1.663 \times 10^{-1} \frac{\sigma^2}{(\mu T)^{1/2}} \sum_{v=0}^{v_{max.}} \left[e^{-\epsilon_v/T} - 1 \right] \text{liters/mole} \tag{74}$$

The σ is now in $\mathring{A}$., the μ in atomic mass units, and the ϵ_o in units of ^oK. The σ and ϵ_o were obtained from Hirschfelder, et al., (13) and the "quantum" values from second virial coefficients were used when given. K was calculated for each double molecule considered, the energy levels found, and the sum (equation 71) taken. The potential parameters for the halogen atoms were taken to be identical to those of the corresponding rare gas atoms. Table 12 gives the calculated quantum equilibrium constants and the corresponding classical quantities found by Bunker and Davidson (19).

The two values of K are in surprisingly good agreement for the stronger bound double molecules. For the more weakly bound double molecules, the quantum values are somewhat less than the classical values, but the differences are negligible for halogen atom recombination rate calculations. At lower temperatures, the differences would become greater. The double molecule of helium-helium was also examined, assuming that there is one bound state near the top of the potential. The classical equilibrium constant is twice the quantum value, although the quantum value is directly proportional to the location of that single bound state.

Table 12

Equilibrium Constants for Double Molecules at 50°C.

Double Molecule	ϵ_o °K.	K	ν max.	K(quantum)	K(classical)
He-He	10.22	0.603	0*	1.19×10^{-4}	2.69×10^{-4}
He-F	19.1	0.233	1	7.50×10^{-4}	7.73×10^{-4}
He-Cl	35.4	0.149	2	2.97×10^{-3}	3.02×10^{-3}
He-Br	41.8	0.127	2	4.22×10^{-3}	4.22×10^{-3}
He-I	47.5	0.109	2	6.60×10^{-3}	6.67×10^{-3}
H_2-I	90.5	0.105	3	2.05×10^{-2}	2.06×10^{-2}
D_2-I	90.5	0.0745	4	2.06×10^{-2}	2.06×10^{-2}
Ne-I	38.6	0.0364	9	**	1.86×10^{-2}
A-I	164.	0.0185	14	**	6.73×10^{-2}

*May be that no bound state exists for He-He.
**Not calculated.

REFERENCES

1. E. Rabinowitch and W. C. Wood, J. Chem. Phys. 4, 497 (1936).

2. D. Britton, N. Davidson, W. Gehman, and G. Schott, J. Chem. Phys. 25, 804 (1956).

3. R. Marshall and N. Davidson, J. Chem. Phys. 21, 659 (1953).

4. K. E. Russell and J. Simons, Proc. Roy. Soc. A 217, 271 (1953).

5. M. I. Christie, R.G.W. Norrish, and G. Porter, Proc. Roy. Soc. A 216, 152 (1953).

6. M. I. Christie, R.G.W. Norrish, and G. Porter, Disc. Faraday Soc. No. 17 (1954), p. 107.

7. M. I. Christie, R.G.W. Norrish, and G. Porter, Proc. Roy. Soc. A 231, 446 (1955).

8. R. L. Strong, J.C.W. Chien, P. E. Graf, and J. E. Willard, J. Chem. Phys. 26, 1287 (1957).

9. D. L. Bunker and N. Davidson, J. Am. Chem. Soc. 80, 5085 (1958).

10. D. L. Bunker, Thesis, California Institute of Technology, 1957.

11. "International Critical Tables," National Academy of Sciences, Maple Press Company, York, Pa., 1933.

12. "Selected Values of Chemical Thermodynamic Properties," National Bureau of Standards, Washington, D.C., 1954.

13. J. O. Hirschfelder, C. F. Curtiss, and R. B. Bird, "Molecular Theory of Gases and Liquids," John Wiley and Sons, Inc., New York, N.Y., 1954.

14. W. E. Henderson and W. C. Fernelius, "Inorganic Preparations," McGraw-Hill, New York, N.Y., 1935, p. 72.

15. R. E. Huffman, Thesis, California Institute of Technology, 1958, p. 26.

16. E. P. Wigner, J. Chem. Phys. 5, 720 (1937); 7, 646 (1939).

17. E. Rabinowitch, Trans. Faraday Soc. 33, 283 (1937).

18. O. K. Rice, J. Chem. Phys. 9, 258 (1941).

19. D. L. Bunker and N. Davidson, J. Am. Chem. Soc. 80, 5090 (1958).

20. D. L. Bunker, private communication.

21. J. Keck, "Research Report 20," AVCO Research Laboratory, April 15, 1958; J. Chem. Phys. 29, 410 (1958).

22. D. E. Stogryn and J. O. Hirschfelder, "The Contribution of Bound, Metastable, and Free Molecules to the Second Virial Coefficient," Wis-Onr-32, N7onr-28511, Univ. of Wisconsin, March 15, 1958.

23. G. Porter and J. A. Smith, "The Recombination of Atoms," Final Technical Report, U.S. Army Contract DA-91-508-EUC-271, ASTIA Document No. 211443, December, 1958.

24. J. A. Magnuson and J. H. Wolfenden, J. Chem. Phys. 60, 1665 (1956).

25. L. I. Katzin and R. L. McBeth, J. Chem. Phys. 62, 253 (1958).

26. R. S. Mulliken, private communication.

27. F. T. Wall, L. A. Hiller, Jr., and J. Mazur, J. Chem. Phys. 29, 255 (1958).

28. F. T. Wall, J. Chem. Phys., to be published.

29. G. Herzberg, "Molecular Spectra and Molecular Structure. I. Spectra of Diatomic Molecules," D. Van Nostrand Co., New York, 1950.

30. R. Taylor, Thesis, California Institute of Technology, 1959.

31. H. Margenau and G. M. Murphy, "The Mathematics of Physics and Chemistry," D. Van Nostrand Co., New York, 1956, p. 486.

32. S. Gill, Proc. Cambridge Phil. Soc. 47, 96 (1951).

33. J. H. Sullivan, private communication.

34. L. I. Schiff, "Quantum Mechanics," McGraw-Hill, New York, N. Y., 1955, Ch. VII.

35. H. Margenau and G. M. Murphy, op. cit., p. 97.

36. Ibid., p. 478.

37. T. Kihara, Rev. Mod. Phys. 27, 412 (1955).

38. J. E. Kilpatric$_{\wedge}^{K}$ and M. F. Kilpatric$_{\wedge}^{K}$, J. Chem. Phys. 19, 930 (1951).

39. D. Britton, to be published.

Propositions

1. Monofluoroacetylene has been prepared recently in high yield (1) and is relatively stable in the gas phase. A study of the gas phase decomposition is suggested, since there is a possibility of obtaining C_2 radicals at relatively low temperatures. Methyl fluoroacetylene and other substituted fluoroacetylenes may undergo some interesting reactions.

2. A study of the thermal reaction kinetics between nitric oxide and hydrogen iodide is proposed. Preliminary observations indicate that this reaction is quite slow at room temperature in the absence of air. Small quantities of air seem to catalyze this reaction.

3. Nitrosyl iodide is not known, but it may exist during iodine atom recombination in the presence of nitric oxide. A method is suggested to obtain the spectrum of nitrosyl iodide in the visible or near ultraviolet.

4. The thermal isotopic exchange of iodine with methyl iodide in the gas phase yields a rate (2):

$$R = k\,[CH_3I]\,[I_2] + k_1\,[CH_3I]$$

The first term is attributed to a CH_3I_3 intermediate complex and the second term is thought to be an exchange initiated by methyl radicals formed on the walls. The addition of small quantities of nitric oxide should eliminate the second term if methyl radicals or iodine atoms are involved.

5. The simplest ketimines are not known, although the higher ketimines are relatively stable (3,4). Methods are proposed to prepare and identify $CH_2 = NH$ and other simple ketimines.

6. The shock tube has been used to study the dissociation rates of iodine in the presence of various third body gases (5). A shock tube investigation of iodine dissociation in the presence of nitric oxide is proposed, since the recombination rate is probably too fast to be easily measured by the flash photlysis method. Bromine recombination in the presence of nitrogen dioxide would also be interesting since nitryl bromide is not known.

7. The "quantum" equilibrium constant for the reaction:

$$I + M \underset{}{\overset{K}{\rightleftharpoons}} IM$$

where IM is bound by a Lennard Jones potential, has been calculated in this thesis by assuming the rotational energy levels given by the rigid rotor approximation. The correct rotational energy

level spacings can be obtained by the use of perturbation theory and the correct equilibrium constant obtained.

8. The remaining unknown oxyhalides of nitrogen are (6) nitryl iodide, nitryl bromide, nitrosyl iodide, and the halogen nitrates (with the exception of FNO_3). It is proposed that some of these might be prepared and identified by trapping them in an inert gas matrix at very low temperatures.

9. The photolysis and thermal kinetics of nitromethane have been studied over a wide range of temperatures (20-480°K.) with various mechanisms being indicated. (7, 8) The high temperature kinetics would be of interest for extrapolation to the conditions prevailing in the detonation of nitromethane. A shock tube investigation of nitromethane is suggested to provide rates and mechanisms more suited to applications in detonations.

References

1. W. J. Middleton and W. H. Sharkey, J. Am. Chem. Soc. 81, 803 (1959).

2. H. Schmied and R. W. Fink, J. Chem. Phys. 27, 1034 (1957).

3. J. B. Culberson, J. Am. Chem. Soc. 73, 4818 (1951).

4. P. L. Pickard and G. W. Polly, J. Am. Chem. Soc. 76, 5169 (1954). (Other papers in a series listed here.)

5. D. Britton, N. Davidson, W. Gehman, and G. Schott, J. Chem. Phys. 25, 804 (1956).

6. D. M. Yost and H. Russell, "Systematic Inorganic Chemistry," Prentice-Hall, New York, 1944. p. 41.

7. H. W. Brown and G. C. Pimentel, J. Chem. Phys. 29, 883 (1958).

8. A. Makovsky and L. Lenji, Chem. Rev. 58, 627 (1958).